ANTIBACTERIAL ACTIVITIES OF CRUDE *Curcuma longa* EXTRACT
MEDIATED SILVER NANO PARTICLES AGAINST ISOLATES FROM
DIABETIC PATIENTS WITH FOOT INFECTIONS

BY

ISAH, Rahmat Mummy
MTech/SLS/2017/7018

A THESIS SUBMITTED TO THE POSTGRADUATE SCHOOL,
FEDERAL UNIVERSITY OF TECHNOLOGY, MINNA, NIGERIA.
IN PARTIAL FULFILLMENT OF THE REQUIREMENTS FOR THE AWARD
OF THE DEGREE OF MASTER OF TECHNOLOGY (M.Tech) IN
MICROBIOLOGY (PHARMACEUTICAL MICROBIOLOGY)

SEPTEMBER, 2021

ABSTRACT

Curcuma longa are traditionally used for the treatment of ulcers, hepatic disorder, wound healing and boost glucose control. This study assessed the phytochemical compositions (quantitative and qualitative), antibacterial activities of *C. longa* crude extracts, synthesis and characterisation of silver nanoparticles, antibacterial activity of extract-mediated silver nanoparticles and wound activity of EeaAgNPs. The antibacterial activity of crude extracts and extract mediated silver nanoparticles (AgNPs) of *C. longa* rhizomes were evaluated against isolates from patients with diabetic foot infection using agar well diffusion method. Quantitative determination of phytoconstituents revealed a significant amount of phytates (6577.9 mg/100 g), cyanides (2741.8 mg/100 g) and saponins (618.0 mg/100 g). Cold maceration of rhizome with 70% ethanol yielded a crude extract (E). Successive partitioning of extract E with chloroform and ethyl acetate yielded chloroform (Ec), ethyl acetate (Eea) soluble fractions, as well as aqueous residual fraction (Eaq). Qualitative screening of the extract and fractions revealed the presence of flavonoids, reducing sugars, anthraquinones, tannins and saponins. The extract and its fractions at 100 mg/ml were inactive on *Pseudomonas aeruginosa, Escherichia coli, Klebsiella pneumoniae, Streptococcus pyogenes* and *Staphylococcus aureus* while, fraction Eea at 200mg/ml was active on *P. aeruginosa, E. coli* and *S. pyogenes*. The wavelength of E-AgNPs, Ec-AgNPs, Eea-AgNPs, and Eaq-AgNPs were 405 nm, 406 nm, 409 nm and 410 nm respectively. The FTIR indicated the presence of aromatic, alkanes, alkynes, alkenes and carboxylic functional groups while the SEM micrograph of Eea-AgNPs revealed clustered rod-like morphology. The highest XRD peak was at 2Θ (34^0). The Eea-AgNPs at 200 mg/ml was active on *S. pyogenes, P. aeruginosa, E. coli* and *K. pneumoniae* with zones of inhibition of 7 ± 1.7 mm, 10 ± 0.7 mm, 11 ± 1.1 mm and 14 ± 0.5 mm respectively. The MIC of Eea-AgNPs against test isolates was at 12.5 mg/ml. The extract was bacteriostatic on the test isolates. There was significant ($P<0.05$) wound closure observed in rats (groups 1 to 6) topically treated with Eea-AgNPs ointment from Day 0 (1.24 ± 0.00 mm to 1.29 ± 0.19 mm) to Day 14 (0.4 ± 0.1 mm to 0.73 ± 0.00 mm) compared to group 7 (Diabetes + Wound only) with (1.23 ± 0.00 to 1.1 ± 0.3 mm). Histology of the treated rats indicated wound healing characterized with collagens, fibroblasts, inflammatory cells, new blood vessels, granulation tissues and complete epithelialization. The application of ointment on rats produced no allergic reactions, rashes and other forms of skin irritation. These findings showed the potentials of *C. longa* as a safe therapeutic agent to treat and heal infected ulcer.

TABLE OF CONTENTS

Content   **Page**

CHAPTER TWO

CHAPTER THREE

CHAPTER FOUR

LIST OF TABLES

LIST OF FIGURES

LIST OF PLATES

LIST OF EQUATIONS

LIST OF ABBREVIATIONS

Abbreviation	Meaning
$AgNO_3$	Silver Nitrate solution
AgNPs	Silver Nanoparticles
AIDS	Acquired Immunodeficiency Syndrome
ANOVA	Analysis of Variance
BA	Blood agar
DFI	Diabetic Foot Infection
DFU	Diabetic Foot Ulcer
DM	Diabetes mellitus
DMRT	Duncan's multiple range test
E	Ethanol extract
E-AgNPs	Ethanol fraction extract-mediated Silver Nanoparticles
Eaq	Aqueous fraction
Eaq-AgNPs	Aqueous fraction-mediated Silver Nanoparticles
Ec	Chloroform fraction
Ec-AgNPs	Chloroform fraction-mediated Silver Nanoparticles
EDX	Energy Dispersive X-ray
Eea	Ethyl acetate fraction
Eea-AgNPs	Ethyl acetate fraction-mediated Silver Nanoparticles
EMBA	Eosine methylene blue agar
EPS	Extra-cellular Polymeric Substances
ESC	Extract Sterility Control
FTIR	Fourier Transform Infrared Spectroscopy
GI	Gastrointestinal Tract

HIV	Human Immunodeficiency Virus
KIA	Kligler Iron Agar
MIC	Minimum Inhibitory Concentration
MBC	Minimum Bactericidal Concentration
MCA	MacConkey agar
MDR	Multi-drug resistant
MRSA	Methicillin resistant *Staphylococcus aureus*
NPs	Nanoparticles
OVC	Organism Viability Control
PUS	Purulent secretions
SEM	Scanning Electron Microscopy
STEC	Shiga toxin-producing *E. coli*
UTIs	Urinary Tract Infections
UV-VIS	Ultraviolet-Visible Spectroscopy
VP	Voges–Proskauer
WHO	World Health Organization
XRD	X-ray Diffraction

LIST OF APPENDICES

CHAPTER ONE

1.0   **INTRODUCTION**

1.1   Background to the Study

Diabetes mellitus (DM) is a complex metabolic disorder characterized by hyperglycemia, pancreatic beta (*β*) cells dysfunction, and abnormal lipid profile that result from metabolic deregulations, impaired insulin secretion and action, and inappropriate consumption of glucose (Iftikhar *et al.,* 2020). Diabetes foot infection is ulceration of tissues of the foot associated with neuropathy disease in a person with diabetes mellitus (Netten *et al.,* 2019).

Diabetic foot infection (DFI) is one of the diabetic complications associated with major morbidity, mortality, and reduced quality of life and is the most serious complication of diabetes mellitus and one of the main problems in health systems and a global public health threat that has increased dramatically over the past two decades (Abdissa *et al*., 2020). According to epidemiological studies, the number of patients with diabetes mellitus increased from about 30 million cases in 1985, 177 million in 2000, 285 million in 2010, and it is estimated that if the situation continues, more than 360 million people by 2030 will have diabetes mellitus (Yazdanpanah *et al*., 2015; Alhubail *et al.,* 2020; Sharma *et al.,* 2021).

Global prevalence of diabetes is high and still on the rise. The prevalence's in the world, Africa, and Nigeria stand at 8.8 %, 3.2 %, and 4.6 %, respectively. An increase in the prevalence of diabetes is accompanied by an increase in its complications such as foot ulcers and lower extremity amputations, in that, the lifetime risk of a person with diabetes developing a foot ulcer is 25 % (Ambrose and Christopher, 2019). The risk for lower extremity amputation is 15 to 40 times higher in people with diabetes than people without diabetes. The complications of diabetes result in reduced quality of life, incapacity and

death. With regard to diabetic foot ulcers, 12 % of all hospitalized diabetic patients in Africa have foot ulceration. Research indicates that diabetes patients with foot ulcers encounter stigma, loss of social role, social isolation, and unemployment. Diabetic foot ulcer is a costly and debilitative disease with severe consequences in diabetic patients. Also, mortality after lower extremity amputations in diabetes patients varies from 39 % to 80 % in 5 years (Ambrose and Christopher, 2019). More than half of all non-traumatic lower limb amputations are due to diabetes. Limb amputation causes distortion of body image, increase in dependency, loss of productivity, and increase in costs of treating diabetic foot ulcers (Ambrose and Christopher, 2019).

Risk factors for the development of DFIs include neuropathy, peripheral vascular disease, and poor glycemic control. In sensory neuropathy, there is diminished perception of pain and temperature. Autonomic neuropathy can cause diminished sweat secretion resulting in dry, cracked skin that facilitates the entry of microorganisms to the deeper skin structures. In addition, motor neuropathy can lead to foot deformities, which lead to pressure-induced soft tissue damage. Peripheral artery disease can impair blood flow necessary for healing of ulcers and infections. Hyperglycemia impairs neutrophil function and reduces host defenses. Trauma in patients with one or more of these risk factors precipitates the development of wounds that can be slow to heal and predispose to secondary infection (Vasanthan *et al*., 2018).

Diabetic foot infections are frequent clinical problems. Infection in foot wounds may be defined clinically by the presence of inflammation or purulence, and then classified by severity. Many organisms, alone or in combinations, can cause DFI, but Gram-positive cocci, especially staphylococci, are the most common (Vasanthan *et al*., 2018). The impaired micro-vascular circulation in patients with diabetic foot limits the access of phagocytes favoring development of infection. *Escherichia coli, Proteus spp.*

Pseudomonas spp., Staphylococcus aureus and Enterococcus spp. are the most frequent pathogens contributing to methicillin-resistant *Staphylococcus aureus* (MRSA) has been commonly isolated from 10 – 40 % of the diabetic progressive and widespread tissue destruction. The increasing association of multi-drug resistant (MDR) pathogens with diabetic foot ulcers further compounds the challenge faced by the physician or the surgeon in treating diabetic ulcers without resorting to amputation (Gunasekaran, 2017).

The known sore infection is predictive of poor ulcer repair and amputation. Proper diagnosis of infection and antibiotic therapy in diabetic foot infections is necessary to ameliorate the yields, because wrong application of antibiotics can lead to resistance and side effects. Three principal factors, such as particular agents, route of administration and duration of remedy may reduce efficacy on the antibiotic therapy of Diabetic foot infection (Abolghasemi and Mesri, 2019).

Curcuma longa (commonly known as turmeric) is also known as Atale pupa by Yorubas, Gangamau by the Hausas, Ohu boboch in Igbo, Girgir by the Tivs. Turmeric is an herbaceous plant of the family Zingiberaceae that has been considered an important therapeutic agent in Indian and Chinese traditional medicine, it is mainly cultivated in tropical and subtropical regions. Turmeric contains curcumin which has therapeutic potential against neurodegenerative disorders, cardiovascular diseases, wound healing ability, hepatic damage, renal diseases and diabetes mellitus (Rashid *et al*., 2017; Rivera-Mancia *et al*., 2018).

Local medicinal uses of turmeric include the use of its herbal decoction with traditional distilled gin called "ogogoro" and it is consumed with the claim that it cures ailments like diabetes, ulcers, hepatic disorders and cough. The rhizome is also used as anti-inflammatory therapy for wounds, digestive disorders and jaundice in babies (Oghenejobo *et al.,* 2017).

The identification of curcumin as the main constituent of turmeric has led to its multiple usage. Pharmacological activities of curcumin (the main active principle in turmeric) include antimicrobial, anti-diabetic, anti-inflammatory, and antioxidant More excitingly, when combined with other drugs, curcumin has been found to enhance the effects of antibacterial, antifungal, anticancer, and antioxidant activities, Curcumin usually exhibit low to no toxicity at the active doses (Sin-Yeang *et al*., 2016). The range of beneficial effects of curcumin in diabetes mellitus and its complications has been attributed to its ability to interact with many key molecules and pathways involved in the pathophysiology of this disease (Rivera-Mancia *et al*., 2018).

In order to enhance the efficacy of *Curcuma longa* extract the need to introduce a nanotechnology system was adapted which is aimed at developing an environmentally friendly and cost-effective approach to synthesise green silver nanoparticles (AgNPs) from silver precursors. This was accomplish using various extracts of turmeric powder, in which the plant biomaterials were used as a reducing as well as capping agent (Alsammarraie *et al*., 2020).

Nanotechnology can be defined as the formation, development, enhancement and exploration of nano sized materials having size range of (1 - 100 nm) that confers them their unique physicochemical properties. It works with the substance which has specific properties such as physical, chemical and biological (Garg and Garg, 2018). Thus, nanotechnology offers an alternative to overcome infectious diseases through the use of antimicrobial nanomaterials (Hernandez *et al*., 2017). Silver nanoparticles (AgNPs) is one of the most used nanomaterials in medical products such as bandages, wound dressings, catheters and textiles due to their excellent microbicidal activity against wild and nosocomial strains of MDR microorganisms (Salomoni *et al*., 2017).

The use of nanotechnology for phytotherapy or treatment of various diseases by herbal medicines, including herbal drug delivery where current and emerging nanotechnologies could enable entirely novel classes of therapeutics has been reported. Interestingly, pharmaceutical sciences are using nanoparticles to reduce toxicity and side effects of drugs. The biologically synthesized nanoparticles with plant products have better chemotherapeutic effects against microbial diseases (Divakaran *et al*., 2018).

Biosynthesis of AgNPs can be accomplished by physical, chemical, and green synthesis; however, synthesis via biological precursors has shown remarkable outcomes. In available reported data, these entities are used as reducing agents where the synthesized nanoparticles are characterized by ultraviolet-visible and Fourier-transform infrared spectra and X-ray diffraction, scanning electron and transmission electron microscopy (Ahmad *et al*., 2020).

1.2 Statement of the Research Problem

Diabetes foot ulcers and infection lead to substantial morbidity and mortality, pains, skin discoloration, abnormal leucocyte function, and deformity which may lead to partial or whole leg amputation, resulting in severe disability, reduced quality of life and high health cost (Nicolas *et al*., 2017; Salutini *et al.,* 2020). Treatment of DFU remains often challenging and time consuming due to the reported uncomfortable outcomes from both surgical and non-surgical procedures (Smith-Strom *et al*., 2017). Drug such as amoxicillin, amoxicillin clavulanic acid, ciprofloxacin, dicloxacillin, flucloxacillin, vancomycin and gentamycin are broad spectrum antibiotics used in the treatment of DFI but have side effects that include hypoglycemia, diarrhea, gastrointestinal alteration, weight loss, nephrotoxicity and nausea (Nicolas *et al.,* 2017).

1.3   Justification for the Research

During the last decades, research has aimed at developing effective therapeutic strategies against diabetic foot infections. Medicinal plants have been used as first line therapy for inflammations, burns, ulcers and surgical wound owning to the fact that they contain natural bioactive compounds which help hasten the process of wound healing and regenerate tissue at the wound site. In an attempt to reduce the side effects of drugs and host of other problems associated with DFI, the medicinal properties of *Curcuma longa* extract and isolated compounds was investigated for their antimicrobial properties against isolates from patients with DFI.

Data generated from this research has contributed to the knowledge of antimicrobial effectiveness on turmeric and validate the traditional claim of the existing data on turmeric as remedy for diabetic foot infection.

1.4   Aim and Objectives

1.4.1   Aim of the study

The aim of the study was to evaluate the antibacterial activity of turmeric (*Curcumin longa*) extract mediated silver nanoparticles against isolates from patients with diabetic foot infection.

1.4.2   Objectives

The objectives of the study were to:

   i.   screen crude extracts of *Curcuma longa* for the presence of various phytochemical components.

  ii.   evaluate antibacterial potentials of crude extracts and extract mediated silver nanoparticles on isolates from patients with diabetic foot infection.

 iii.   determine the minimum inhibitory concentrations (MIC) and minimum bactericidal concentrations (MBC) of extract mediated silver nanoparticles.

iv.   characterize extract mediated silver nanoparticles.

v.   carry out topical toxicological study in rats.

CHAPTER TWO

2.0   **LITERATURE REVIEW**

2.1   **Description of *Curcuma longa***

Curuma longa (Turmeric) botanically related to ginger (Zingiberaceae family), is a perennial plant having a short stem with large oblong leaf and bears ovate, pyriform or oblong rhizomes, which are often branched and brownish-yellow in colour (Choudhury, 2019). It is one of the largest family of rhizome plants with approximately 80 species spread throughout tropical and subtropical regions of the world. It is an annual perennial plant with leafy and erect stem. It thrives well where there is no much rainfall under mild condition of warm and humid atmosphere. It has leaves with thin blades. It has an ovate sheath-like long petiole with entire margin. Turmeric rhizome is yellow in colour and this colour is due to the presence of the curcumin, which is crystalline and insoluble in water but soluble in solvents like ethanol, acetone, ketone and chloroform. Turmeric has a peculiar smell which is reported to be due to the aromatic volatile oil components present. This oil component contains 25 % tumerone, 11.5 % curdine and 8.55 % ar-turmerone (Oghenejobo *et al.,* 2017). Turmeric is spread throughout tropical and subtropical regions of the world that are generally cultivated in Asia countries, mainly in India and China (Chanda and Ramachandra, 2019). Table 2.1 summarizes the taxonomy of *Curcuma longa*.

Table 2.1: Taxonomy of *Curcuma longa*

Taxonomic Group	Plant
Kingdom	Plantae
Subkingdom	Tracheobionta
Super division	Spermatophyta
Division	Magnoliophyta
Subclass	Zingiberidae
Order	Zingiberales
Family	Zingiberaceae
Genus	*Curcuma*
Species	*longa*
Scientific name	*Curcuma longa*

Source: Chanda and Ramachandra (2019).

2.2   Local Medicinal Uses of *Curcuma longa*

In herbal and traditional medicine, turmeric is used for rheumatoid arthritis, conjunctivitis, skin cancer, small pox, chicken pox, wound healing, urinary tract infections (UTI) and various digestive disorders among other conditions (Rathore *et al.,* 2020). Turmeric also helps to cure liver disease, cancer, atherosclerosis, and osteoarthritis, menstrual problem, bacterial infection, and eye disorder (Roshan and Gaur, 2017).

Locally turmeric is used as a decoction with traditional distilled gin called "ogogoro" and it is consumed with the claim that it cures ailments like diabetes, ulcers, hepatic disorders and cough. The rhizome is also used as anti-inflammatory therapy for wounds, digestive disorders and jaundice in babies (Oghenejobo *et al.,* 2017). Turmeric boosts glucose control and augments the effects of the medications which are used in the treatment of

diabetes. It also lowers the body's resistance to insulin which can prevent Type-2 diabetes from developing (Verma *et al.,* 2018). Turmeric has lots of benefits for the skin including speeding up the process of healing wounds, calming pores on the face to reduce acne. Since it has antioxidant and anti-inflammatory properties, which is use for treating skin problems (Verma *et al.,* 2018; Chanda and Ramachandra, 2019). Because of its antiseptic and antibacterial properties, turmeric has been used as wound healing agent. The topical application of curcumin found in turmeric aids in wound healing by supporting granulation tissue formation, collagen deposition, tissue remodeling and wound contraction (Krebs-Holm *et al.,* 2020).

2.3   Phytochemistry of *Curcuma longa*

Rhizomes of *Curcuma longa* contain several active secondary metabolites that play major role in the array of bioactivity attributed to it. These secondary metabolites include alkaloids, anthraquinone, cardiac glycosides, coumarins, polyphenolics, reducing sugars, saponins, sesquiterpene lactones, steroids, steroid glucoside compounds and terpenoids (Sawant and Godghate, 2020).

Phytochemical investigation of turmeric has revealed it contains curcuminoids and volatile oils as the major components. Curcumin and two dimethoxy derivatives, desmethoxycurcumin and bisdemethoxycurcumin, are the major curcuminoids in turmeric, which have anti-cancer, anti-inflammatory, neuroprotective, anti-Alzheimer's and anti-oxidant activities. Curcuminoids have always been the focus of drug research (Chao *et al.,* 2018).

2.4   Diabetic Foot Infection

Diabetic foot infection (DFI) is diagnosed clinically on the basis of the presence of purulent secretions (pus) or at least two (2) of the cardinal manifestations of inflammation; redness, warmth, swelling or induration, and pain or tenderness (Boulton

et al., 2018). Other features that have also been associated with DFI include: glucose level ≥ 250 mg/dl, non-purulent secretions, necrosis, friable granulation tissue, undermining of wound edges and foul odour (Mills *et al*., 2019). There are two principal approaches to the diagnosis of DFU infections: microbiological and molecular approaches (Ramirez-Acuna, *et al*., 2019).

2.4.1 Microbiological approaches: It is crucial to isolate the causative microorganisms of DFI to engage in appropriate treatment. Four major techniques are used to collect samples from deep tissue wounds. These techniques include needle aspirates, swabs, a tissue biopsy (the most advantageous and standard method), and curettage after debridement. Due to the fear of infectious growth and the loss of adjacent ischemic or healthy tissue, biopsies are a very difficult and delicate procedure. On the other hand, swab cultures are manageable since sample collection becomes easier and can be taken from any kind of wound. However, swab cultures are sometimes not reliable since they generally include the colonizing but not the causative pathogens. Traditional wound swab cultures do not correlate well with tissue biopsy cultures and often lead to overuse and non-directed antimicrobial therapy, incrementing bacterial multi-resistance. Therefore, sample collection techniques play a crucial role in bacterial culture identification (Ramirez-Acuna, *et al*., 2019).

2.4.2 Molecular approaches: Molecular biology tools provide a powerful means to define microbial communities in chronic wounds. Significant microbial diversity can be revealed in a single clinical sample by using culture-free sequencing of bacterial DNA. The identification of the bacterial micro biome was made possible by the discovery of the 16S ribosomal DNA sequence, known as "the universal primer". The identification of bacterial DNA is carried out by the amplification and sequencing of 16S DNA. Then, a comparison is made between the identified flanking sequences and a group of known

bacterial sequences from a virtual library, which then determine the bacterial species; with some standards, it is possible to estimate the bacterial load. One of the most important advantages that molecular approaches have over traditional bacterial cultures is the time spent in bacterial identification, because the detection of microbes is possible on the same day the sample is collected, without the time required for bacterial growth in a culture or the environmental selection pressures inherent to the culturing processes. Molecular methods are progressing and becoming more accessible and affordable. It is now possible to use bacterial DNA from a wound site to identify the pathogens present. Hence, this method should be available for most of the diabetic community, to enable a better microbial assessment of wounds (Ramirez-Acuna, *et al*., 2019).

2.5   Pathogenesis

The diabetic foot ulcer, DFU mostly appears to be polymicrobial in nature (Sindhu, 2018). Both Gram-positive (*S. aureus*, *Enterococcus*) and Gram-negative (*P. aeruginosa, E. coli, Klebsiella spp, Proteus spp*) are involved in DFU. These organisms combine together and form micro-communities within a matrix of extra cellular polymeric substances, EPS and this is termed as biofilm (Alvarado-Gomez *et al.,* 2017). The percentage of dominance for biofilm formation by each organism varies, the biofilm formation was dominated by *Pseudomonas* spp which was then followed by species of *Corynebacterium, Acetinobacter, Staphylococcus* and then *Enterococcus*. Vestby *et al*. (2020) reported that the predominant biofilm former was *S. aureus* followed by *P. aeruginosa*, *Citrobacter spp*, *E. coli*, *Proteus spp* and then *Klebsiella oxytoca*. It was found that polymicrobial communities was able to produce higher biofilm formation than individual species (Vestby *et al.,* 2020).

2.6   Global Epidemiology

The life time risk of DFU in a person living with diabetes is 15 % but it could be up to 25 %. The annual incidence is around 3 %. The geographical variation in the prevalence is related to the prevalence of diabetes as well as sociocultural factors that enhance the occurrence. Also important are the socioeconomic standard and access to quality health care (Ibrahim, 2018).

A recently published systematic review and meta-analysis by Zhang *et al*. (2017) of studies from various continents indicated that Belgium had the highest prevalence globally (16.6 %). The global prevalence of DFU was 6.3 % and was higher in type 2 diabetes (6.4 %) than type 1 diabetes (5.5 %). The prevalence in Belgium was followed by Canada (14.8 %) and the United States (13.0 %). North America had the highest continental prevalence of 13 %. Africa was 7.2 %, Asia 5.5 % and Europe 5.1 %. Among European countries, the prevalence in Norway was 10.4 %, Italy was 9.7 % and Poland 1.7 %. In Asia, India had a prevalence of 11.6 %, Thailand 8.8 % and Korea 1.7 %. Finally, in Africa the prevalence in Cameroun was 9.9 %, Egypt 6.2 %, South Africa 5.8 % and Uganda 4 % (Zhang *et al*. 2017).

A systematic review on the prevalence of DFU in five Arab countries indicated that Saudi Arabia had a mean prevalence of 11.85 %, Egypt had 4.2 % and that of Jordan was 4.65 %. Also, the prevalence in Bahrain was 5.9 % and 2.7 % in Iraq (Mairghani *et al.,* 2017). A Report by DanMusa *et al*. (2016) from a study conducted in a tertiary hospital in Northwestern Nigeria, revealed a DFU prevalence of 6 % which is close to the global average. In the same study 67.2 % of patients were males while 32.8 % were females (DanMusa *et al*., 2016).

2.7 Treatment

2.7.1 Debridement

Debridement is the removal of the bacterial biofilm and necrotic tissue from a wound and is one of the key components of foot ulcer infection treatment. It facilitates the complete assessment of the wound, provides tissue for microbiological culture, and promotes wound healing (Ramirez-Acuna, *et al.*, 2019).

2.7.2 Surgery

Many DFIs require surgical intervention, varying from local incision and debridement to high level amputation, depending on the severity of infection and degree of peripheral vascular disease. The goal of surgery is to control the infection while preserving maximal function and quality of life and the level of amputation is determined by the extent and severity of the infection (Mills *et al.,* 2019).

2.7.3 Wound care

The wound bed should be managed to promote healing. In addition to debridement, strategies include inspection, cleansing, surface debris removal, and wound protection. Wound debridement should be used to remove non-viable tissue in the wound bed and stimulate a granular wound bed (Mills *et al.*, 2019).

2.7.4 Topical antimicrobials

Topical antimicrobials are not a preferred treatment for chronic wounds due to their lack of contribution to moisture balance maintenance and autolytic debridement, as well as the potential for the development of contact dermatitis. When used, topical antimicrobials are selected base on their low toxicity to the host tissue (Ramirez-Acuna, *et al.*, 2019). Some topical antiseptics/antimicrobials available for DFIs are:

i. Chlorhexidine; this agent has a broad antibacterial effect and promotes wound healing. However, it may damage cartilage tissue (Ramirez-Acuna, *et al.*, 2019).

ii. Acetic acid; this is a useful treatment against bacteria from the *genus Pseudomonas* and other Gram-negative bacteria. It can produce tissue toxicity and cause fibroblast growth inhibition (Ramirez-Acuna, *et al.*, 2019).

iii. Silver compounds; foams, calcium alginates, hydro fibers, hydrogels, sheets, silver sulfadiazine cream, and silver nitrate sticks produce activities against *E. coli, Klebsiella* spp*, S. aureus,* and methicillin-resistant *Staphylococcus aureus* (MRSA), and also have antifungal and antiviral properties (Ramirez-Acuna, *et al.*, 2019).

iv. Hydrogen Peroxide; this type of peroxide has activities against Gram-positive bacteria. Its main adverse effect is a risk of bullae formation (Ramirez-Acuna, *et al.*, 2019).

2.8 Prevention

2.8.1 Lifestyle modification

It is crucial to emphasize that diabetic foot is a diabetic complication. Hence, the lifestyle modifications that are required to prevent or manage diabetes e.g., diet and exercise represent an integral component of every strategy necessary to prevent diabetic foot complication. Exercise is one of the most common lifestyle requirements in diabetes and it improves tissue perfusion that is required for wound healing. It is also reported to enhance wound size reduction in DFU (Ibrahim, 2018).

2.8.2 Medications

Intensive control of blood glucose is required to prevent both macrovascular and microvascular complications. Adequate treatment of hypertension and dyslipidemia is essential to prevent vascular complications (Ibrahim, 2018).

2.9 Medical Significance of Some Diabetic Foot Infection Pathogens

2.9.1 *Pseudomonas aeruginosa*

Pseudomonas aeruginosa is a Gram-negative opportunistic pathogen and a model bacterium for studying virulence and bacterial social traits. While it can be isolated in low numbers from a wide variety of environments including soil and water, it can readily be found in almost any human and animal-impacted environment. It is a major cause of illness and death in humans with immunosuppressive and chronic conditions, and infections in these patients are difficult to treat due to a number of antibiotic resistance mechanisms and the organism's propensity to form multicellular biofilms. It is member of the genus *Pseudomonas*, colloquially called the pseudomonads. The water-soluble pigments, pyocyanin and pyoverdin, give the organism its distinctive blue-green colour on solid media. *Pseudomonas aeruginosa* produces indophenol oxidase, an enzyme that renders them positive in the "oxidase" test, which distinguishes them from other Gram-negative bacteria (Diggle and Whiteley, 2020). Like many environmental bacteria, *P. aeruginosa* live-in slime-enclosed biofilms, which allow for survival and replication within human tissues and medical devices. It is associated with the production of a biofilm that protects it from host-produced antibodies and phagocytes contributing to antibiotic resistance of this organism. The organism thrives in moist environments such as soil and water. It can be found in large numbers on fresh fruits and vegetables. Human colonization begins within the gastrointestinal tract, with subsequent spread to moist cutaneous sites such as the perineum and axilla. They are difficult organisms to eradicate

from areas that become contaminated, such as operating and hospital rooms, clinics and medical equipment (Diggle and Whiteley, 2020).

Pseudomonas aeruginosa is an important plant pathogen, affecting lettuce, tomatoes and tobacco plants. It can be found in freshwater environments (streams, lakes, and rivers), as well as sinks, showers, respiratory equipment, even contaminating distilled water (Poulsen *et al*., 2019). Human beings can ingest the *P. aeruginosa* from such sources; however, it does not adhere well to normal intact epithelium. Therefore, it may be found as part of normal intestinal flora, and with a healthy immune system, does not cause infection. It is involved in a variety of human infections ranging from neonatal sepsis, to burn sepsis, and acute and chronic lung infections. This organism is a common opportunistic pathogen, leading to infections in patients with defects in host defenses, such as chronic neutropenias and defects of neurtrophil function, hematologic cancers, Human Immunodeficiency (HIV)/acquired immunodeficiency syndrome (AIDS) and Diabetes mellitus (Freschi *et al*., 2019).

2.9.2   *Streptococcus pyogenes*

Streptococcus pyogenes is a Gram-positive bacterium, also referred to as group A streptococcus*,* is a common human pathogen that causes a wide variety of diseases, including infections of the throat, skin and a toxic shock syndrome with high mortality. Like many other bacterial pathogens, *S. pyogenes* expresses surface proteins that show great structural variability between strains, a variability that probably allows the bacteria to avoid the immune system of the host (Thern *et al*., 2020).

Streptococcus pyogenes is one of the most successful human pathogens, and clearly its vast arsenal of virulence factors has enabled it to cope with all immune defences of the human body. The organism primarily colonises the epithelial surface of the nasopharynx and skin and, in most cases, results in asymptomatic carriage. Under certain conditions

and observed more frequently in specific serotypes, *S. pyogenes* can cause a suite of diseases, from superficial to life-threating infections, as well as post-infection immune-related diseases. It expresses a broad variety of surface-bound virulence factors, allowing it to efficiently escape immune recognition and prevent phagocytic uptake. One of the most prominent and well-studied virulence factors of *S. pyogenes* are the M-proteins and M-related proteins (Laabei and Ermert, 2019).

Streptococcus pyogenes infections cause diverse clinical manifestations ranging from mild and common local infections such as tonsillitis, impetigo and erysipelas to life-threating systemic disease like sepsis and meningitis (Karlsson *et al*., 2018).

2.9.3 *Klebsiella pneumoniae*

Klebsiella pneumoniae is a Gram-negative bacterium belonging to the Enterobacteriaceae family. This microorganism is part of the healthy microbiome of individuals and colonizes many parts of the body. Despite its role as a healthy component of the microbiome, it can cause severe infections in critically ill patients, newborns, immunocompromised individuals or those with other risk factors in healthcare establishments (Reyes *et al*., 2019). The organism has recently gained notoriety as an infectious agent due to a rise in the number of severe infections and the increasing scarcity of effective treatments. These concerning circumstances have arisen due to the emergence of *K. pneumoniae* strains that have acquired additional genetic traits and become either hypervirulent (HV) or antibiotic resistant. *Klebsiella* spp are often resistant to multiple antibiotics. Current evidence implicates plasmids as the primary source of the resistance genes (Paczosa and Mecsas, 2016).

Typical *K. pneumoniae* is an opportunistic pathogen that is widely found in the mouth, skin and intestines, as well as in hospital settings and medical devices. Opportunistic *K. pneumoniae* mostly affects those with compromised immune systems or who are

weakened by other infections. Colonization of the gastrointestinal tract (GI) tract by opportunistic *K. pneumoniae* generally occurs prior to the development of nosocomial infections, and *K. pneumoniae* colonization can be further found in the urinary tract, respiratory tract and blood. The biofilms that form on medical devices (e.g., catheters and endotracheal tubes) provide a significant source of infection in catheterized patients. Nosocomial infections caused by *K. pneumoniae* tend to be chronic due to the two following major reasons: *K. pneumoniae* biofilms formed *in vivo* protect the pathogen from attacks of the host immune responses and antibiotics; and nosocomial isolates of *K. pneumoniae* often display multidrug-resistance phenotypes that are commonly caused by the presence of extended-spectrum β-lactamases or carbapenemases, making it difficult to choose appropriate antibiotics for treatment (Davarci *et al*., 2019).

2.9.4 *Escherichia coli*

Escherichia coli is a Gram-negative bacilli of the family Enterobacteriaceae. They are facultative anaerobes and nonsporulating. *Escherichia coli* strains with the K_1 capsular polysaccharide antigen cause approximately 40 % of cases of septicemia and 80 % of cases of meningitis (Makvana and Krilov, 2015). *Escherichia coli* is a bacterium that is commonly found in the gut of humans and warm-blooded animals. Most strains of *E. coli* are harmless. Some strains however, such as Shiga toxin-producing *E. coli* (STEC), can cause severe foodborne disease. It is transmitted to humans primarily through consumption of contaminated foods, such as raw or undercooked ground meat products, raw milk, and contaminated raw vegetables and sprouts (WHO, 2018).

Phylogenetically, *E. coli* is a member of the Enterobacteriaceae and is closely related to pathogens such as *Salmonella*, *Klebsiella*, *Serratia*, and the infamous *Yersinia pestis*, which causes plague. Although *E. coli* is mostly harmless, pathogenicity islands have been identified and associated with pathogenesis in *E. coli* resulting in strains that

colonize different tissues. The building blocks of *E. coli* consists of about 55 % protein, 25 % nucleic acids, 9 % lipids, 6 % cell wall, 2.5 % glycogen, and 3 % other metabolites, which for biotechnological applications is important, since carbon flux is often a problematic issue to address in order to generate a novel metabolic pathway or to enhance a current functioning pathway. Also, carbon flux is tightly regulated by sophisticated regulatory networks that require modeling and a basic understanding of the regulatory mechanisms in order to manipulate them and achieve desired goals (Nauru-Idalia and Bernardo, 2017).

2.9.5 *Staphylococcus aureus*

Staphylococcus aureus is a Gram-positive non-motile, non-spore forming facultative anaerobe that is biochemically catalase and coagulase positive (Bitrus *et al*., 2018)**.** *Staphylococcus aureus* is a ubiquitous bacterial pathogen that can perfectly adapt and is capable of living in different states. It has been reported that *S. aureus* can survive in an inanimate environment, existing as a colonizer or commensal, and may form biofilms. It is an important cause of a wide range of clinical infections including bacteraemia and infective endocarditis, osteoarticular, skin and soft tissue, pleuropulmonary, and device-related infections (Bshabshe *et al*., 2020).

Clinically, *S. aureus* is the most pathogenic member of the genus staphylococci and the etiologic agent of a wide variety of diseases that ranges from superficial skin abscess, food poisoning and life-threatening diseases such bacteremia, necrotic pneumonia in children and endocarditis. The severity of the disease is due to the production of several putative virulence factors and possession of antibiotic resistance genes such as staphylococcal exotoxins and other factors that facilitates the initiation of disease process, immune evasion and host tissue destruction (Bitrus *et al*., 2018).

Staphylococcus aureus (including drug-resistant strains such as MRSA) are found on the skin and mucous membranes, and humans are the major reservoir for these organisms. It is estimated that up to half of all adults are colonized, and approximately 15 % of the population persistently carry *S. aureus* in the anterior nares. Some populations tend to have higher rates of *S. aureus* colonisation (up to 80 %), such as health care workers, persons who use needles on a regular basis (*i.e.,* diabetics and intravenous (IV) drug users), hospitalized patients, and immunocompromised individuals. The organism can be transmitted from person-to-person by direct contact or by fomites (Taylor and Unakal, 2019).

2.10   Importance of Silver Nanoparticles (AgNPs)

Nanoparticles (NPs) are structures smaller than 100 nm. Nanotechnology is a branch of technology that examines the properties of these structures (Baran and Acay, 2019). Nanotechnology is a rapidly growing field with its application in science and technology for the purpose of manufacturing novel materials at the nanoscale level. It is a multidisciplinary field which employs techniques from diverse disciplines. Nanoparticles exhibit special features like large surface area, quantum effect and ability to bind and carry compounds like drugs. The physical, chemical, optical and electronic properties of the nanoparticles depend on the size, shape and surface morphology (Rajsekhar *et al*., 2015).

Nanoparticles are considered a bridge between atomic structures and bulk size of materials. Moreover, inorganic nanoparticles have unique features due to their small size and large surface to-mass ratio. Different types of metallic nanoparticles have been prepared, including gold and silver nanomaterials that have gained considerable attention due to their high performance in many scientific fields, such as optics, catalysis, and biosensing. In particular, silver nanoparticles (AgNPs) have been used as an excellent

antimicrobial and antioxidant agent and as a catalyst for accelerating some chemical reactions. Silver nanoparticles biosynthesized from aqueous silver nitrate through a simple and eco-friendly route using *Curcuma longa* tuber-powder extracts act as a reductant and stabilizer simultaneously (Alsammarraie *et al*., 2018).

The surging popularity of green methods has triggered synthesis of AgNPs using different sources, like bacteria, fungi, algae, and plants, resulting in large-scale production with less contamination. Plant phytochemicals show greater reduction and stabilization. *Eugenia jambolana* leaf extract was used to synthesize AgNPs that indicated the presence of alkaloids, flavonoids saponins, and sugar compounds. Phenolic compounds of pyrogallol and oleic acid were reported to be essential for the reduction of silver salt to form NPs. Pepper-leaf extract acts as a reducing and capping agent in the formation of AgNPs of 5 – 60 nm. Some other reductants used for plant mediated synthesis of AgNPs (AgNO$_3$) are polysaccharide, soluble starch, natural rubber, tarmac, cinnamon, stem-derived callus of green apple, red apple, egg white, lemon grass, coffee, black tea, and *Abelmoschus esculentus* juice (Ahmad *et al.,* 2019).

Nanotechnologies as drug delivery systems are designed to improve the pharmacological and therapeutic properties of conventional drugs. The drugs are transported to the target site without accumulation in any site by using nanoparticles. The nanotechnology improves bioavailability of drugs, efficiency and selectivity as well as reduces the side effects and toxicity. Reduction of plasma fluctuation and higher solubility plays a vital role in drug delivery. Various nanoparticles are used to deliver drugs such as polymeric miscalls, polymeric nanoparticles, polymeric drug conjugates, nanocrystals and lipid-based nanoparticles like liposomes and solid lipids (Wanigasekara and Witharana, 2016). Inorganic nanoparticles like metal nanoparticles (Gold, Silver, Iron, Platinum, Quantum dot) and silica nanoparticles (mesoporous xerogels). The drugs are binded to the

nanoparticles by help of different conjugations like encapsulation, non-covalent complexation and conjugation to polymeric carrier via liable linkers. The drug conjugate nanoparticles enter to the cell by passive or active targeting, respectively by diffusion or by receptor mediated endocytosis. Finally, nanoparticles can release drugs in response to enzymes or pH changes. Nanoparticles based drug delivery still develop to cure diseases such as cancer, diabetes, heart diseases and central nerve diseases (Wanigasekara and Witharana, 2016).

CHAPTER THREE

3.0   MATERIALS AND METHODS

3.1   Study Area

Whole rhizomes of turmeric were collected from Kure Ultra-modern Market Minna, Chanchaga Local Government Area, Niger State, Nigeria in the month of July, 2019. Chanchaga local government area is one of the 25 local government areas in Niger State with its headquarters in Minna the state capital as shown in Figure 3.1 below. It is situated at 9.62^0 North latitude, 6.54^0 East Longitude and 294 m above sea level (GIS, 2021).
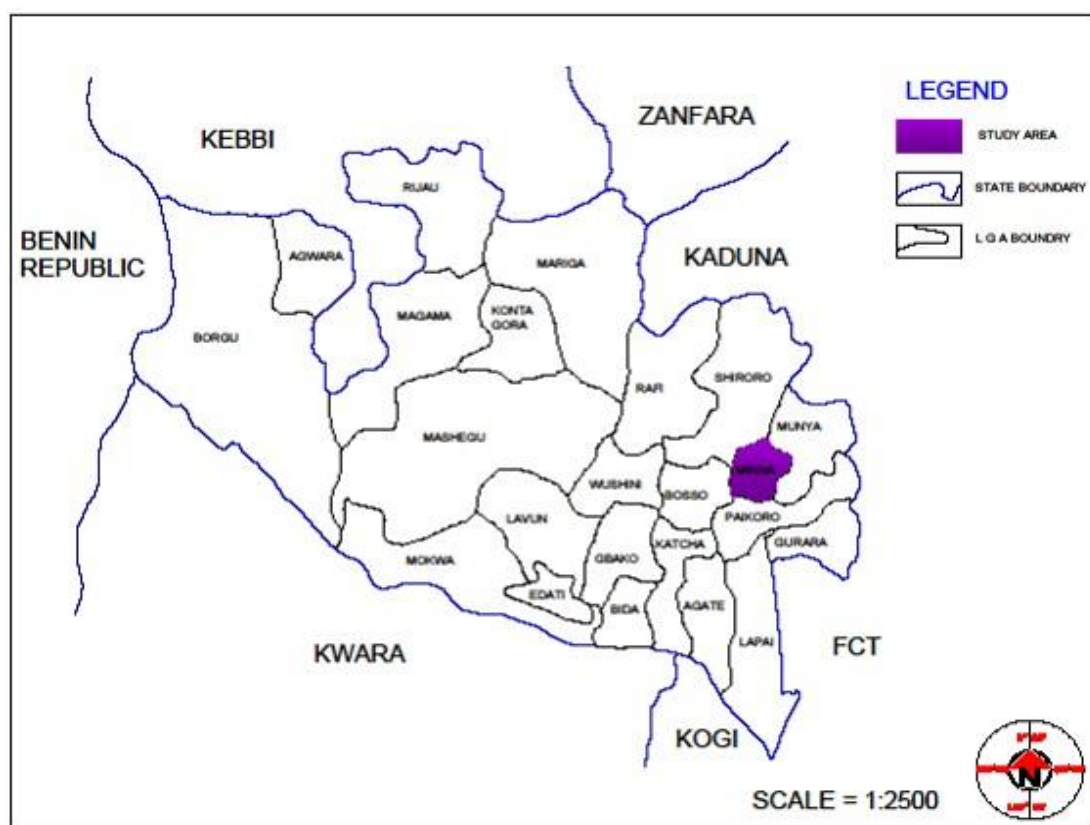
Figure 3.1: Map of Niger State Showing Study Area; Chanchaga Local Government Area
(General Hospital Minna, Niger State)
Source: Geographical information system laboratory (GIS, 2021).

3.2 Collection and Identification of Plant Material

Fresh and healthy rhizomes of turmeric were transferred into sterile plastic bag and transported to the Laboratory of the Department of Biological Sciences, Federal University of Technology, Minna for identification by an ethnobotanist, Dr A.Y.O. Daud. It was identified as *Curcuma longa*. Voucher specimen were preserved in the department for future reference. Plates I and II show the pictures of the sample.

Plate I: Rhizomes of *Curcuma longa* (Source: Field work)

Plate II: Powder of *Curcuma longa* (Source: Field work)

3.3 Preparation and Extraction of Plant Material

The method of Egas *et al.* (2020) was employed in the preparation of *C. longa* for extraction. The plant rhizomes were cut into small pieces and freeze-dried using RE-6000 rotary evaporator and FGJ-18 freeze dryer at temperature between -30 °C to -50 °C for three days. The freeze-dried rhizomes of *C. longa* were pounded with mortar and pestle and pulverised to powered form with an electric blender (Kenwood CG100, 750 watt). The pulverised sample were labeled and stored in a sterile container. Patil *et al.* (2021) method was employed for the extraction which was carried out in the Vaccine and Drug Discovery Laboratory, Centre for Genetic Engineering and Biotechnology, Federal University of Technology Minna.

Cold maceration of two hundred grams (200 g) of pulverized *C. longa* powder with 70 % ethanol (1000 mL) yielded a crude ethanol extract (coded E). Successive and exhaustive partitioning of extract E with chloroform (150 mL) and ethyl acetate (150 mL) gave rise to chloroform (coded Ec), ethyl acetate (coded Eea) soluble fractions as well as aqueous residual fraction (coded Eaq). The crude extract and fractions were freeze dried and weighed. The resulting weight were 25 g for crude ethanol, 19 g for chloroform fraction, 17 g for ethyl acetate fraction and 10 g aqueous residual fraction respectively. The percentage recovery for extract and fraction were calculated and recorded in % as shown in equation 3.1 below. All extract/fractions were stored in a well labelled air tight sample bottles at 4 °C until required for use.

$$\text{Percentage recovery} = \frac{\text{weight of obtained extract}}{\text{weight of plant material}} \text{ X } 100 \qquad (3.1)$$

3.4 Phytochemical Screening of Extract and Fractions *Curcuma longa* Rhizomes

Phytochemical screening was carried out on all the four extracts of the plant to detect the presence or absence of various secondary metabolites (alkaloids, saponins, flavonoids,

tannins, phenolic acids) using standard method (Bahar *et al*., 2018; Umar *et al.,* 2020; Muhammad and Fathuddin, 2021).

3.4.1   Test for saponins

Five milliliters (5 mL) of distilled water were added to 0.2 g of each *C. longa* rhizome extract in a test tube and agitated vigorously for 2 minutes. Persistent frothing or form indicate the presence of saponins.

3.4.2   Test for alkaloids

Two-point five milliliter (2.5 mL) of 1 % aqueous HCl were added to 0.2 g of each *C. longa* rhizome extract and placed over a water bath for 30 minutes and filtered. The individual filtrates were then treated with few drops of Wagner's reagents. A deep-brown creamy precipitate confirmed a positive test for alkaloids (Bahar *et al.,* 2018).

3.4.3   Test for anthraquinones

Zero-point two grams (0.2 g) of each *C. longa* rhizome extract were treated with 10 cm^3 of chloroform and agitated for 5 minutes, and 10 % ammonia (NH_3) solution was added to the chloroform. A brick red precipitate in the upper layer indicated the presence of anthraquinones.

3.4.4   Test for flavonoids

Few drops of aqueous NaOH and few drops of HCL were treated with 2mL of plant extract. Formation of yellow colour indicates the presence of flavonoid (Hassan *et al.,* 2017).

3.4.5   Test for sterols

Each *C. longa* rhizome extract (0.2 g) were treated with 2 cm^3 of chloroform and 3 cm^{3}of concentrated sulphuric acid (H_2SO_4) to form a layer. A Reddish-brown colouration at interface confirmed the presence of steroids (Bahar *et al.,* 2018).

3.4.6   Test for tannins

Two-point five milliliter (2.5 mL) of distilled water were added to each *C. longa* rhizome extract (0.2 g), filtered and a few drops of 10 % ferric chloride solution was added to each filtrate. A blue colour indicated the presence of tannins.

3.4.7   Test for phlobatannins

Each *C. longa* rhizome extract (0.2 g) were boiled with 5 cm^3 of 1 % HCl in a test tube. A red precipitate indicated the presence of phlobatannins.

3.4.8   Test for phenols

Each *C. longa* rhizome extract (0.2 g) were treated with 1.0 mL of 10 % ferric chloride solution. A deep-bluish green solution indicated the presence of phenols.

3.4.9   Proteins

Xanthoproteic test: extract was treated with few drops of concentrated HNO_3 formation of yellow which indicates the presence of proteins (Bahar *et al.,* 2018).

3.4.10   Reducing sugar

Benedict's test: filtrate was treated with Benedict's reagent and heated gently, orange red ppt indicates the presence of reducing sugar (Bahar *et al.,* 2018).

3.5   Sample Size

The sample size was determined using the Fisher's formular and 130 samples were employed in the study.

$$n = \frac{Z^2\ Pq}{d^2} \qquad\qquad (3.2)$$

where n = sample size

Z = critical value at 95% confidence level usually set at 1.96

P = prevalence (8.8% prevalence was used) base on previous studies

q = 1 – P

d = precision i.e. degree of freedom 5 %

$Z^2 = 1.96$

$P = 8.8 \% = 0.088$

$q = 1 - 0.088 = 0.912$

$d = 5 \% = 0.05$

$$n = \frac{(1.96)^2(0.088)(0.91)}{(0.05)^2}$$

$n = 123.05 \approx 123$

The sample size was increased to 130.

3.6   Collection of Test Organisms

Ethical approval was obtained from research and ethics committee of General Hospital and IBB Specialist Hospital, Minna, Niger State. Consent forms were duly filled by patient/patient guidance before sample collection. Specimen were collected from diabetic patients with foot ulcers by swabbing directly at the base of the infected wound, swabs were taken intra-operatively at the deepest part of the wound. The specimens were obtained using sterile commercially purchased swabs and stored in sterile normal saline containers and was transported immediately in ice pack box to Center for Genetic Engineering and Biotechnology, Minna.

3.7   Isolation of Test Organisms

 The modified method of Abdallah *et al*., (2018) was adopted. The swabs were cultured on nutrient agar and incubated at 37 ℃ for 24 h and subsequently characterised by sub-culturing onto eosine methylene blue agar (EMBA), blood agar (BA) and MacConkey agar, the organisms isolated includes; *Klebsiella pneumoniae, Escherichia coli, Pseudomonas aeruginosa, Staphylococcus aureus and Streptococcus pyogenes.* The organisms were then maintained on nutrient agar slants until required for use (Abdallah *et al*., 2018).

3.8   Identification and Characterization of Test Organisms

The isolates were characterized using biochemical tests (Bello, 2018; Abdallah *et al.,* 2018). The resulting colonies were Gram stained and further characterized using standard biochemical tests (motility test, catalase, urease, oxidase, nitrate reduction, indole, hydrogen sulphide production, haemolysis production, sugar fermentation tests, methyl red test, citrate test and Voges-proskauer test). The results of the biochemical tests were compared with that of known taxa.

3.8.1   Gram staining

Gram staining was carried out according to the procedure described by Rave *et al.* (2019). Grease-free glass slides were used to prepare a thin smear of the pure 24 h old culture, fixed by passing over a flame and the slides were placed on the staining rack. The smear was covered with 2 drops of crystal violet stain and left for 60 seconds and rinsed carefully under running water. The smear was flooded with Gram's iodine solution and left for 30 seconds and rinsed with water, slides were decolorized with 70 % alcohol for 15 seconds and rinsed with water then drained completely. The slides were finally counterstained with 2 drops of safranin for 60 seconds and rinsed with water until no color appears in the effluent then the slides were blotted dry with absorbent paper and observed under oil-immersion objective lens (x100) microscope. Gram-positive bacteria appeared dark purple while Gram-negative bacteria appeared pale to dark red.

3.8.2   Motility test

From fresh overnight liquid cultures, a straight wire loop was used to inoculate tubes containing motility medium by stabbing straight half way the tubes. The inoculated tubes were incubated at 37 °C for 24 h. The tubes were observed for the presence or absence of growth along the line of stab. Motile bacteria grew a long line of stab and diffused into

the medium with turbidity while non-motile bacteria grew only along the line of stab and did not diffuse into the medium with no turbidity (PHE, 2015).

3.8.3   Oxidase test

Colonies from 24 h cultures were placed on filter papers and a drop of oxidase reagent was added onto each filter paper and examined within 10 seconds. Oxidase-positive bacteria developed bluish-purple colour while oxidase-negative bacteria did not develop blue colour (Rave *et al*., 2019).

3.8.4   Catalase test

A sterile wire loop was used to pick colonies from 24 h cultures onto dry glass slides. A drop of 3 % H_2O_2 was placed on each glass slide and observed for the evolution of air bubbles. Catalase-positive bacteria produced copious active bubbling while catalase negative bacteria produced few bubbles or none (Rave *et al*., 2019).

3.8.5   Coagulase test

All isolates were tested for coagulase test using human plasma serum. Two drops of saline water were taken onto the slide and mixed with the bacterial sample. A drop of serum was added on the saline drop and mixed well. The slide was rocked gently for about 10 seconds. Positive test was indicated by clumping of bacterial cells in the plasma within 10 seconds. Failing to form bacterial cells clump indicates a negative result for coagulase test (Begum *et al.,* 2017).

3.8.6   Urease test

The surface of urea agar slants was streaked with 24 h broth cultures. The cap of the tubes was left on loosely and incubated at 37 ^0C for 48 h then examined for colour change. Urease positive-bacteria developed a magenta to bright pink colour in 24 h while urease-negative bacteria did not develop colour change (Rave *et al*., 2019; Alhubail *et al.,* 2020).

3.8.7 Citrate utilization test

Inocula picked from the centre of a well-isolated colony of 24 h cultures were streaked on slant tubes containing Simmon citrate agar. The slant tubes were incubated at 37 °C for up to 4 days and observed for colour change along the slants. Bacteria that utilized citrate showed growth with colour change from green to intense blue along the slants while bacteria that did not utilize citrate showed no growth and no colour change (slants remained green) (Rave *et al*., 2019).

3.8.8 Hydrogen sulphide production test

Inocula picked from colonies of 24 h bacterial cultures were inoculated in tubes containing Kligler iron agar (KIA) by straight stabbing to a depth of 2 cm. The tubes were incubated at 37 °C for 48 h and the tubes were observed for colour change for H_2S production. Bacteria that produced hydrogen sulphide turned the medium black while bacteria that did not produce hydrogen sulphide do not turn the medium black (Rave *et al*., 2019).

3.8.9 Methyl red test

Prior to inoculation, the medium was allowed to equilibrate to room temperature. Inocula from 24 h bacterial cultures were transferred into tubes containing MR medium. The tubes were incubated at 37 °C for 24 h. Following 24 h of incubation, 1 mL of the broth was transferred into each clean test tube. The remaining broth were reincubated for an additional 24 h. Methyl red indicator 2 drops was added to each aliquot and observed for colour change immediately. Red colour indicated positive reaction while yellow colour indicated negative reaction (Rave *et al*., 2019).

3.8.10 Voges–proskauer test

Prior to inoculation, the VP medium were allowed to equilibrate to room temperature. Inocula from 24 h bacterial cultures were inoculated in the tubes containing VP medium.

The tubes were incubated at 37 ℃ for 24 h. Following 24 h of incubation, 1 mL of the broth was dispensed into each clean test tube. The remaining broth were reincubated for an additional 24 h. Six drops of 5 % alpha-naphthol were added to each aliquot and homogenized. Two drops of 40 % potassium hydroxide were added to each aliquot and agitated. The tubes were agitated vigorously for 30 min and observed for colour change. A pink-red colour at the surface of the tubes indicated a positive reaction while absence of pink-red colour at the surface of the tubes indicated a negative reaction (Rave *et al.*, 2019).

3.8.11 Indole test

Test tubes containing 4 mL of tryptophan broth each were sterilized. The tubes were inoculated aseptically with inoculum from 24 h bacterial cultures. The tubes were incubated at 37 ℃ for 48 h. Kovac's reagent (0.5 mL) were added to each broth culture and observed for the presence or absence of ring. Formation of a pink to red colour (cherry-red ring) in the reagent layer on top of the medium within seconds of adding the reagent indicated a positive reaction while no colour change indicated a negative reaction (Rave *et al.,* 2019).

3.8.12 Sugar fermentation test

  i.   **Lactose fermentation**

Inocula from 24 h bacterial cultures were transferred aseptically to sterile tubes of phenol red lactose broth. The inoculated tubes were incubated at 37 ℃ for 24 h and observed for colour change. A colour change from red to yellow indicated a positive reaction while no colour change indicated a negative reaction (Rave *et al.,* 2019).

34

ii. Sucrose fermentation

Inocula from 24 h bacterial cultures were transferred aseptically to sterile tubes of phenol red sucrose broth. The inoculated tubes were incubated at 37 °C for 24 h and observed for colour change. A colour change from red to yellow indicated a positive reaction while no colour change indicated a negative reaction (Rave *et al.,* 2019).

iii. Glucose fermentation

Tubes of glucose fermentation medium were inoculated with inocula from 24 h bacterial cultures using a straight wire by stabbing half way to the bottom of the tubes. One tube of each pair was covered with 1 cm layer of sterile mineral oil or liquid paraffin (creates anaerobic condition in the tube by preventing diffusion of oxygen). The other tubes were left open. All tubes were incubated at 37 °C for 48 h, up to 4 days and observed for colour change in the medium. Acid production was detected in the medium by colour change from green to yellow, which indicated glucose fermentation while no colour change indicated a non-glucose fermentation (Rave *et al.,* 2019).

iv. Fructose fermentation

Inocula from 24 h bacterial cultures were transferred aseptically to sterile tubes of phenol red fructose broth. The inoculated tubes were incubated at 37 °C for 24 h and observed for colour change. A colour change from red to yellow indicated a positive reaction while no colour change indicated a negative reaction (Rave *et al.,* 2019).

3.8.13 Haemolysis production test

Inocula from 24 h bacterial cultures were inoculated on blood agar plates. The plates were incubated at 37 °C for 24 h and observed for the presence of haemolysis. Beta-haemolysis showed complete lysis of red blood cells surrounding the colonies. Alpha-haemolysis showed greenish discolouration of red blood cells surrounding the colonies while gamma-haemolysis showed slight discolouration in the medium (Rave *et al.,* 2019).

3.9 Standardization of Microorganisms

Under aseptic condition, a loopful of 24 h culture of each organism was sub-cultured into 5 ml of sterile nutrient broth and incubated at 37 °C for 24 h. Exactly 0.2 mL of overnight cultures of each organism was dispensed into 20 mL of sterile nutrient broth and incubated for 3 to 5 h to standardize the culture to 10^6 Cfu/mL. The absorbance was determine using spectrophotometer. The range of the readings include 0.07 to 0.10 at a wavelength of 600 nm. The standard cultures were used for the antimicrobial assay (Babayi *et al*., 2018).

3.10 Antibacterial Screening of Crude Extract and Fractions

The crude ethanol extract, ethyl acetate, chloroform, and aqueous fractions of *Curcuma longa* at 100 mg/mL (1 mg content) and 200 mg/mL (2 mg content) were assayed for their antibacterial activities on the test organism using agar well diffusion method as described by Manandhar *et al.,* (2019). A measured quantity of 1.0 g and 2.0 g of each extract/fraction was reconstituted in 10 mL of sterile distilled water for the polar fraction (Aqueous) while for the non-polar and mid-polar extract/fraction (ethanol, ethyl acetate and chloroform) the extract/fractions were first homogenized with 1 mL of each of the solvent (ethyl acetate, chloroform and ethanol) and then 9 mL of sterile water was added. The extract/fractions were stirred and agitated vigorously for homogeneity. Under aseptic condition a loopful of the standardized organisms were inoculated into a solidified sterile Mueller Hinton agar plate and spread with sterile wire loop then a hole with diameter of

6 mm was bored aseptically with a sterile cork-borer and 0.2 mL of each extract/fraction was taken and dispensed into bored holes and incubated for 24 h at 37 ℃. The plates were prepared in triplicates and control plates comprised of medium alone, solvent plus agar and organism, extract sterility control (ESC) and organism viability control (OVC). The efficacy of extract and each fraction was compared with Amoxicillin/Clavulanate (0.5 mg/mL) for each organism.

3.11 Synthesis of Extract and Fraction-mediated Silver Nanoparticles

Silver nanoparticles was synthesized by mixing silver nitrate ($AgNO_3$) solution with different extract/fractions (ethanol, ethyl acetate, chloroform and aqueous) using modified method of Sankar *et al*., (2017). The $AgNO_3$ solution was prepared by dissolving 0.0358 g of $AgNO_3$ in 100 mL distilled water to give 2 mM concentration. The synthesized AgNPs were prepared in the ratio 1:2 (10 mL of extract and 20 mL of $AgNO_3$ solution) and 1:4 (10 mL of extracts and 40 mL of $AgNO_3$ solution). Thereafter, the solution was adjusted to pH 11 and the reactant mixtures were kept under the sun for 10 min. The colour change of the solution was checked periodically within the 10 min.

3.12 Characterisation of Synthesised Silver Nanoparticles

The silver nanoparticles synthesised were characterised using ultraviolet-visible spectroscopy (UV-VIS spec) of the reaction mixture after 24 h of reaction, X-ray diffraction (XRD), Scanning electron microscopy (SEM), Fourier transform infrared spectroscopy (FTIR) and Energy dispersive X-ray (EDX) (Garg and Garg, 2018; Baran and Acay, 2019).

The reduction of pure Ag^+ ions were observed by measuring the UV-Vis spectrum of the reduction media at different time intervals taking 1 mL of the sample, compared with 1 mL of distilled water used as blank. The UV-Vis spectral analysis has been done by using a Perkin Elmer-Lambda 25 UV/Vis spectrophotometer at a resolution of 1 nm from 200

to 1000 nm/mins and absorption peaks were observed and recorded at 400–450 nm regions, which are identical to the characteristics UV-visible spectrum of silver nanoparticles (Shafaghat, 2015). The Fourier transform infrared, FTIR of the synthesized silver nanoparticles solution was achieved by centrifuging at 10000 rpm for 30 min. The pellet was washed thrice with 5mL of deionized water to get rid of the free proteins or enzymes that are not capping the silver nanoparticles and pellet was dried by using vacuum drier and analyzed with Nicolet 800 FTIR spectrometer (Nicolet, Madison, WI, USA). For XRD A thin film of the silver nanoparticle was made by dipping a glass plate in a solution and carried out for X-ray diffraction studies the dry powders of the silver nanoparticles (SNPs) were used, the XRD patterns showed the silver crystalline structure of the synthesised nanoparticles. The diffracted intensities and peaks were recorded from 20° to 90° at 2Θ degree. The SEM micrograph was achieved by preparing Thin films of the sample on a carbon coated copper grid by just dropping a very small amount of the sample on the grid pellet extra solution was removed using a blotting paper sand then the film on the SEM grid was allowed to dry and the morphology and size of silver nanoparticle was evaluated by Philips GM-30 transmission electron microscope (Hillsboro, USA), at an accelerating voltage of 120 kV (Sharifi-Rad *et al*., 2020)

3.13   Antibacterial Screening of the Synthesised Extract and Fractions Mediated Silver Nanoparticles

The antibacterial activity of synthesized silver nanoparticles was investigated against five bacterial isolates. The synthesized AgNPs at 200 mg/mL and 400 mg/mL were assayed for their antibacterial activities using agar well diffusion method (Srirangam and Rao, 2017), 0.8 g of freeze dried AgNPs were dissolved into 4 mL of distilled water to obtain 200 mg/mL concentration while 0.8 g of freeze dried AgNPs were dissolved into 2 mL of distilled water to obtain 400 mg/mL concentration. Under aseptic condition a loopful of

the standardized organism was inoculated into a solidified sterile Mueller Hinton agar plate and spread with sterile wire loop then a hole with diameter of 6 mm was bored aseptically with a sterile cork-borer and 0.2 mL (20 mg/mL and 40 mg/mL) of each synthesized extract was taken and dispensed into bored holes and incubated for 24 h at 37 $^\circ$C. The plates were prepared in duplicates and control plates comprised of medium alone, silver nitrate solution (AgNO$_3$), extract mediated silver nanoparticle and organism viability control (OVC).

3.14 Determination of Minimum Inhibitory Concentration of Extract and Fractions-mediated Silver Nanoparticles

Minimum inhibitory concentration (MIC) of extract mediated silver nanoparticles of ethylacetate, chloroform, ethanol and aqueous of *C. longa* determined against the test isolates at varying concentration of 200 mg/mL, 100 mg/mL, 50 mg/mL, 25 mg/mL, 12.5 mg/mL and 6.25 mg/mL. The MIC of each extract were determined by micro-broth dilution techniques as described by Omeje and Kelechi (2019). A loopful of standardized test organism was inoculated into a sterile test tube of nutrient broth containing two-fold dilution of the synthesised extract and was inoculated at 37 $^\circ$C for 24 h.The MIC was determined by observing the growth in each test tube with different concentrations of extract and by observing the lowest concentration of the extract that inhibited growth of each organism.

3.15 Determination of Minimum Bactericidal Concentration of Extract and Fraction-mediated Silver Nanoparticles

Minimum bactericidal concentration of extract/fraction mediated silver nanoparticles of ethyl acetate, chloroform, ethanol and aqueous of *C. longa* were determined using the method of Omeje and Kelechi (2019). The sterile molten agar was dispensed into Petri dishes and allowed to cool and gelled under aseptic condition the tubes that did not show

any visible growth from MIC above were sub-cultured into freshly prepared sterile nutrient agar and incubated at 37 $^{\circ}$C for 24 h. The plates with least concentration of the extract that showed no growth after 24 h was recorded as MBC.

3.16 Determination of Wound Healing Activity of Ethyl acetate-mediated Silver Nanoparticles.

The method of Wubante *et al.* (2018) was used for this study. A total of fifty (50) healthy Wistar rats (100 - 150 g) were used for this study. The animals were purchased from Animal Farm, University of Ilorin, Kwara State, Nigeria. The rats were kept in clean plastic cages bedded with dry clean wood shaving, maintained at a temperature of (25 ± 2) $^{\circ}$C and observed under 12 h light/dark cycle of prevailing time period in a well-ventilated room and allowed to acclimatize for 2 weeks before the commencement of the experiment. They were fed with standard feeds 'Caps Feed' (Caps Feed Limited, Ibadan, Nigeria) and tap water *ad libitum.* The animal house was cleaned and disinfected regularly. The soiled base wood shavings were replaced often. The feed and water containers were washed regularly. The animals were cared for in accordance with the Guidelines for the Care and the Use of Laboratory Animals of the Institute for Laboratory Animal Research Council, National Research Council, USA (2011).

The rats were divided into 10 groups of 5 animals each. Groups 1 to 7 were starved for 24 h and injected with alloxan monohydrate (150 mg/kgbw) via intraperitoneal route. After 3days of injecting the rats, symptoms such as frequent urination, fatigue, blurred vision, glucose level higher than 250 mg/dl indicated that the rats were diabetic. Groups 7, 8, 9 and 10 were used as control. Laceration of the skin of rats in groups 1 to 9 was done using sterile blade. The wound was allowed to establish for 24 h. Subsequent infection of the wound with the test organisms was done for groups 1 to 6 and left for four days for the infection to establish after which physical observation such as swollen

wound, smelly liquid draining from the wound and rapidly spreading of wound indicated the wound rottening or necrotic phase. Swabbing of the infected wound and subculturing on a fresh agar plate then incubated for 24 h at 37 ^{o}C was done to ensure the growth of similar test isolate. Treatment of wound with ointment in groups 1 to 6 and 9 commenced on the 4th day. The ethyl acetate-mediated silver nanoparticle 2 ml was mixed with 1 g of Vaseline and 4 g of paraffin wax to make an even mixture of ointment (Dons and Soosairaj, 2018). The ointment was applied to groups 1 to 6, 9 and 10 only for 14days. Group 10 rats were not wounded but their hair was shaved and served as control that were administered ointment only. Wound contractions were measured for 14 days at interval of 2 days. The wound contraction was measured using a white thread placed on the wound area measuring from one end to the other end of wound, then placed on a meter rule to determine the size of wound closure. The wound contraction is calculated as:

$$\text{Percentage Wound Closure} = \frac{(\text{wound area on 1st day} - \text{wound area on day (n)})}{\text{Wound area on 1st day}} \times 100 \qquad (3.3)$$

Where n is number of days.

The grouping is shown below:

Group 1: - Diabetes + Wound + *Streptococcus pyogenes* + Ointment

Group 2: - Diabetes + Wound + *Escherichia coli* + Ointment

Group 3: - Diabetes + Wound + *Klebsiella pneumoniae* + Ointment

Group 4: - Diabetes + Wound + *Staphylococcus aureus* + Ointment

Group 5: - Diabetes + Wound + *Pseudomonas aeruginosa* + Ointment

Group 6: - Diabetes + Wound + Mixed organisms + Ointment

Group 7: - Diabetes + Wound only (Negative control)

Group 8: - Wound induction only (Positive control)

Group 9: - Wound induction + Ointment only

Group 10: - Shaved Skin + Ointment

3.17 Histopathology of Wounds

The method Paul *et al*. (2017) was used for histological study of the wounds. The healing tissues from all the groups of animals were obtained on the 15th day and processed for histological study. The skin was washed in normal saline and fixed immediately in 10 % buffered formalin for a period of 24 h. Grossing was achieved by selection of the skin to be processed. The skin was placed on tissue cassette alongside the identification number. The selected skin tissues were processed using automatic tissue processor (SLEE MTP Tissue processor), which involved four major stages; fixation, dehydration, clearing and impregnation. An embedding machine was used to dispense wax into an embedding mould, unto which the processed tissues and tissue cassettes are placed and allowed to solidify. The solidified tissue in the cassette were placed in MR3500 microtome and tiny sections were cut at 5 microns. The tissue sections were flooded on a heated water bath maintained at 3 °C below melting point of the wax. Tissue sections were picked using microscopic slides angled at about 45 °C for water to drain and dry. The slide was then placed on hot plate and allowed to fix at maintained temperature of 3 °C above the melting point of wax. This was done to ensure bond between the tissue and slides and allowed fixing for minimum of 30 min. Thereafter, the slides were stained using Harri's haematoxylin and eosin method and allowed to air dry. The dried slides were mounted with Distyrene Plasticizer Xylene (DPX) mountant and cover slips and examined under the microscope. Any alterations compared to the normal structures were recorded (Paul *et al.,* 2017).

3.18 Statistical Analysis and Data Evaluation

All numeric data generated were expressed as the mean ± standard Error of mean (SEM). Comparison between different groups were performed using analysis of variance

(ANOVA Test). The significant difference between control and experimental groups were assessed using Duncan's multiple range test (DMRT) using SPSS version 19.

CHAPTER FOUR

4.0 RESULTS AND DISCUSSION

4.1 Results

4.1.1 Description of crude ethanol extract/fractions of *Curcuma longa*

Table 4.1 shows the physical appearance and percentage recovery of crude ethanol extract (E), chloroform (Ec), ethyl acetate (Eea) and aqueous (Eaq) fractions of *Curcuma longa*. Chloroform extract had the highest percentage recovery (76 %) followed by ethyl acetate extract (68 %), aqueous extract (40 %) while the crude ethanol extract had the least percentage recovery (12.5%).

Table 4.1: Physical Characteristics and Percentage Recovery of crude ethanol extract and fractions of *Curcuma longa* rhizomes.

Physical Characteristics of extract/fractions					Percentage Recovery (%)
Crude ethanol	E	Reddish Brown	Sticky Paste	25	12.5
Chloroform	Ec	Yellowish	Scrumpsy	19	76
Ethyl acetate	Eea	Reddish	Rocky Paste	17	68
Aqueous	Eaq	Dark Brown	Thicky Paste	10	40

4.1.2 Phytochemical components of crude ethanol extract and fractions of *Curcuma longa*

4.1.2.1 *Qualitative phytochemical components of crude ethanol extract and fractions of Curcuma longa*

The qualitative phytochemical components of crude ethanol extract (E) and chloroform (Ec), ethyl acetate (Eea) and aqueous (Eaq) fractions of *Curcuma longa* are presented in Table 4.2. Reducing sugar and anthraquinones are present in all the extracts of *C. longa* while phenols and proteins are absent. Saponins were present in all the extracts except in

44

chloroform extract. Alkaloids and tannins were absent in all the extracts except in ethanol extract, flavonoids were present in chloroform and aqueous extracts while steroids were present only in aqueous extract.

Table 4.2: Qualitative Phytochemical Components of crude ethanol extract and fractions of *Curcuma longa*

Phytochemical components	Extract/Fractions			
	E	Ec	Eea	Eaq
Saponins	+	ND	+	+
Alkaloids	+	ND	ND	ND
Flavonoids	ND	+	ND	+
Tannins	+	ND	ND	ND
Phenols	ND	ND	ND	ND
Steroids	ND	ND	ND	+
Reducing sugars	+	+	+	+
Anthraquinones	+	+	+	+
Proteins	ND	ND	ND	ND

E: Crude ethanol extract   +: Present

Ec: Chloroform fraction   ND: Not detected

Eea: Ethyl acetate fraction

Eaq: Aqueous fraction

4.1.2.2 *Quantitative phytochemical components*

The quantitative phytochemical components of *curcuma longa* are shown in Table 4.3. The results revealed high concentrations of phytate (6577.9 mg/100 g), cyanides (2741.8 mg/100 g), saponins (618.0 mg/100 g), moderate amount of phenols (158.3 mg/100 g) and low level of alkaloids (40.2 mg/100 g), flavonoids (22.5 mg/100 g), tannins (19.5 mg/100 g) with insignificant amount of oxalate (0.8 mg/100 g).

Table 4.3: Quantitative Phytochemical Components of *Curcuma longa*

Component	Sample quantity (mg/100 g)
Phenols	158.338
Flavonoids	22.58
Alkaloids	40.251
Cyanides	2741.8
Phytate	6577.986
Tannins	19.54
Oxalates	0.870
Saponins	618.004

4.1.3 Characteristics and Identities of Bacterial Isolates

The identities of the test organisms are summarized in Table 4.4. *Pseudomonas aeruginosa, Klebsiella pneumoniae, Escherichia coli, Streptococcus pyogenes* and *Staphylococcus aureus* were isolated from samples collected from patients with diabetic foot infection.

4.1.4 Antibacterial activities of crude ethanol extract and fractions of *Curcuma longa* rhizomes against test isolates

The antibacterial activities of the crude *Curcuma longa* extract against test isolates are shown in Tables 4.5 (at 1 mg content) and 4.6 (at 2 mg content of extract/fractions) respectively. The crude ethanol (E), chloroform (Ec), ethyl acetate (Eea) and aqueous (Eaq) fractions were inactive against *P. aeruginosa, E. coli, K. pnuemoniae, S. pyogenes* and *S. aureus* at 1 mg content and 2 mg content respectively. However, amoxicillin/clavulanate at 0.1 mg content was effective against all the test isolates.

4.1.5 Characteristics of *Curcuma longa* fraction-mediated Silver Nanoparticles

The appearance of dark brown colouration confirmed formation of silver nanoparticles in the solution (Plate III). The UV-Visible spectrum of the synthesised silver nanoparticles of the extracts are shown in Figure 4.1 indicating the absorbance peak for ethyl acetate fraction mediated silver nanoparticles (Eea-AgNPs) occurred at 410 nm. Figure 4.2 shows that the absorbance peak for aqueous fraction mediated silver nanoparticles (Eaq-AgNPs) was at 409 nm. Figure 4.3 indicates that the absorbance peak for ethanol fraction mediated silver nanoparticles (E-AgNPs) was 406 nm, and Figure 4.4 shows that the absorbance peak for chloroform fraction mediated silver nanoparticles (Ec-AgNPs) was 405 nm. All the absorbance peaks are within range for the formation of silver nanoparticles. The FTIR of ethyl acetate fraction mediated silver nanoparticles revealed the possible biomolecules in the region of $1000 - 4000$ cm^{-1} of mediated silver nanoparticles showing functional groups. Figure 4.5 shows the transmission peaks at 3280, 2914, 2847, 2113, 1640, 1203, 1461, 1349, 1148, 928 and 998 cm^{-1}. A broad and strong bend at 3280 cm^{-1} corresponded to O-H stretch of alcohols. The peaks at around 2923 and 2847 cm^{-1} corresponded to C-H stretch of aromatics and -OCH$_3$ groups (alkanes). The bend at 2113 cm^{-1} corresponded to C≡C stretch of alkynes functional groups. The bend at 1640 cm^{-1} was owing to the bend C=C stretch. Peaks appeared at 1203, 1461, 1349 and 1148 cm^{-1} and corresponded

to C-N stretch aromatic amines, N-H bend amines, C-H bend alkanes and C-H bend alkyl halides. Peaks at 928 cm^{-1} corresponded to typical OH bend and N-H wag representing carboxylic acid and 1° and 2° amines and 998 cm^{-1} corresponded to ≡C-H bend representing alkenes group.

Figure 4.6 is the SEM micrograph which formed a rod like morphology and aggregated nanoparticle without any considerable variation from each other. The elemental signals of AgNPs synthesised were analysed by EDX. Figure 4.6 shows that Energy dispersive X-ray (EDX) spectrum exhibited the signal of silver and other elements from synthesised nanoparticles. The EDX spectrum determined the presence of C (61.79 %), O (27.45 %), Na (9.05 %), Si (0.05 %), P (0.15 %), S (0.11), Cl (0.05 %) K (0.97 %) and Ag (0.37 %) peaks at 0.1, 0.2 and 1.0 K$_e$V were assigned to C, O and Na. Si, P, S, Cl, Ag and K elements corresponded to weak signals. The results also confirmed the formation of AgNPs. The crystalline structure of AgNPs determined by XRD at distinct diffraction peaks shown in Figure 4.8 indicated the structure of AgNPs as face-centered cubic and had a similar diffraction profiles with numerous sharp intense peaks at various 2Ө (degree) of 8°, 18°, 27°, 29°, 34°, 37°, 40°, 45°, 53° and 57° which indicated the crystallinity of the EeaAgNPs and also confirmed the formation of silver nanoparticles. The pattern showed strong diffraction peak at 34°. Thus, the XRD formed were crystalline in nature.

Table 4.4: Microscopic, Morphological and Biochemical Characteristics of Bacterial Isolates

GR	SHAPE	COG	OX	MO	CT	IN	MR	VP	CI	UR	H$_2$S	Sugar Fermentation				HAEMOLYSIS			Suspected organisms
												L	S	G	F	α	β	γ	
+	cocci	-	-	-	-	-	-	+	-	-	-	+	+	+	+	-	+	-	*Streptococcus pyogenes*
-	rod	-	-	-	+	-	-	+	+	+	-	+	+	+	-	-	-	-	*Klebsiella pneumoniae*
-	rod	-	+	+	+	-	-	-	+	+	-	+	+	+	-	-	-	+	*Pseudomonas aeruginosa*
+	cocci	+	-	-	+	-	+	+	+	+	-	+	+	+	+	-	+	-	*Staphylococcus aureus*
-	rod	-	-	+	+	+	+	-	-	-	-	+	-	+	-	-	-	-	*Escherichia coli*

GR: Gram's reaction   UR: Urease   γ: Gamma haemolysis production   +: Positive

COG: Coagulase   H$_2$S: Hydrogen Sulphide production   VP: Vogues-Proskauer   -: Negative

OX: Oxidase   NI: Nitrate reduction   CI: Citrate utilization

CT: Catalase   L: Lactose sugar fermentation   α: Alpha haemolysis production

MR: Methyl red   S: Sucrose sugar fermentation   β: Beta heamolysis production

IN: Indole   G: Glucose sugar fermentation   ND: Not determine

Table 4.5: Antibacterial Activities of crude Ethanol extract and fractions of *Curcuma longa* 1 mg Content

Extract/Fractions	Inhibition Zone Diameter (in mm) against Test Isolates				
	Pseudomonas aeruginosa	*Escherichia coli*	*Klebsiella pneumoniae*	*Streptococcus pyogenes*	*Staphylococcus aureus*
Eaq	0.00 ± 0.0^a	0.00 ± 0.0^a	0.00 ± 0.0^a	0.00 ± 0.0^a	0.00 ± 0.0^a
E	0.00 ± 0.0^a	0.00 ± 0.0^a	0.00 ± 0.0^a	0.00 ± 0.0^a	0.00 ± 0.0^a
Eea	0.00 ± 0.0^a	0.00 ± 0.0^a	0.00 ± 0.0^a	0.00 ± 0.0^a	0.00 ± 0.0^a
Ec	0.00 ± 0.0^a	0.00 ± 0.0^a	0.00 ± 0.0^a	0.00 ± 0.0^a	0.00 ± 0.0^a
Control	17 ± 1.0^b	23.3 ± 1.67^b	23 ± 1.15^b	18 ± 1.0^b	19 ± 0.0^b

Values are zone of inhibition mean ± standard error of mean of triplicate determinations. Values with the same superscript in the same column are not significantly different at $P < 0.05$.

Eaq: Aqueous fraction   Mg/mL: milligram per millilitre

E: Ethanol extract   mm: millimeter

Eea: Ethyl acetate fraction   Ec: Chloroform fraction

Table 4.6: Antibacterial Activities of crude Ethanol extract and fractions of *Curcuma longa* crude 2 mg Content

Extract/Fractions	Inhibition Zone Diameter (in mm) against Test Isolates				
	Pseudomonas aeruginosa	*Escherichia coli*	*Klebsiella pneumoniae*	*Streptococcus Pyogenes*	*Staphylococcus aureus*
Eaq	02.60±0.6[b]	0.00±0.0[a]	0.00±0.0[a]	0.00±0.0[a]	0.00±0.0[a]
E	0.00±0.0[a]	0.00±0.0[a]	0.00±0.0[a]	0.00±0.0[a]	0.00±0.0[a]
Eea	5.00±0.5[c]	3.00±0.5[b]	0.00±0.0	5.00±0.57[b]	0.00±0.0[a]
Ec	0.00±0.0[a]	0.00±0.0[a]	0.00±0.0[a]	0.00±0.0[a]	0.00±0.0[a]
Control	17±1.0[d]	23.3±1.6[c]	23±1.15[b]	18±1.0[c]	19±0.0[b]

Values are zone of inhibition mean ± standard error of mean of triplicate determination. Values with the same superscript letters in the same column are not significantly different at P < 0.05.

Eaq: Aqueous fraction   Mg/mL: milligram per millilitre

E: Ethanol extract   mm: millimeter

Eea: Ethyl acetate fraction

Ec: Chloroform fraction

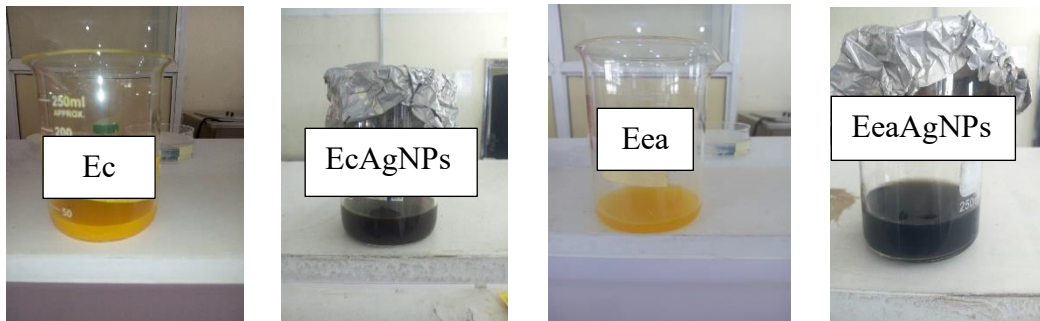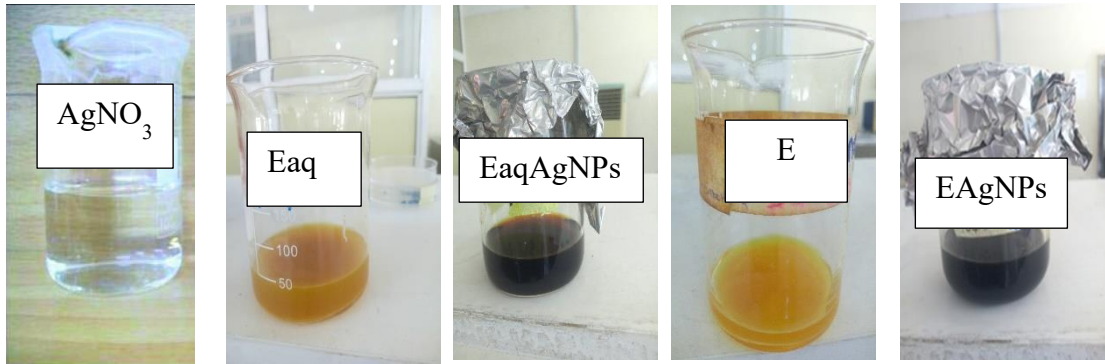Plate III: Colour changes before and after synthesis of nanoparticles

AgNO$_3$ – Silver nitrate solution

Eaq – Aqueous fraction

Eaq-AgNPs – Aqueous fraction mediated silver nanoparticles

E – Crude ethanol extract

E-AgNPs – Ethanol fraction extract mediated silver nanoparticles

Ec – Chloroform fraction

Ec-AgNPs– Chloroform fraction mediated silver nanoparticles

Eea – Ethyl acetate fraction

Figure 4.1: UV- Visible Spectrum of Ethyl acetate fraction mediated Silver Nanoparticles
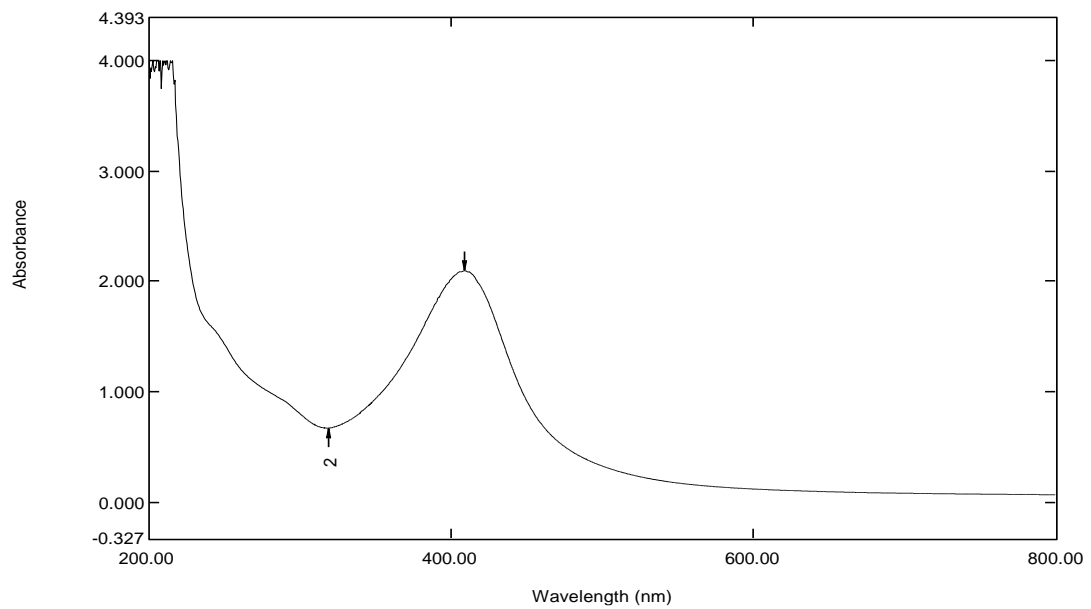
Figure 4.2: UV- Visible Spectrum of Aqueous fraction mediated Silver Nanoparticles

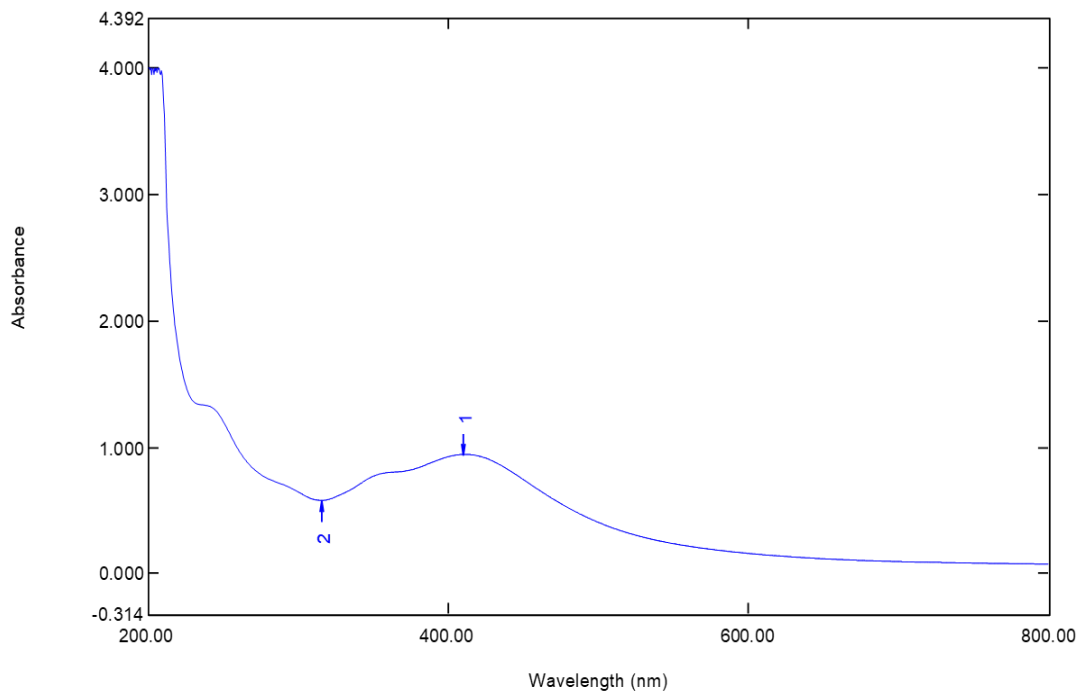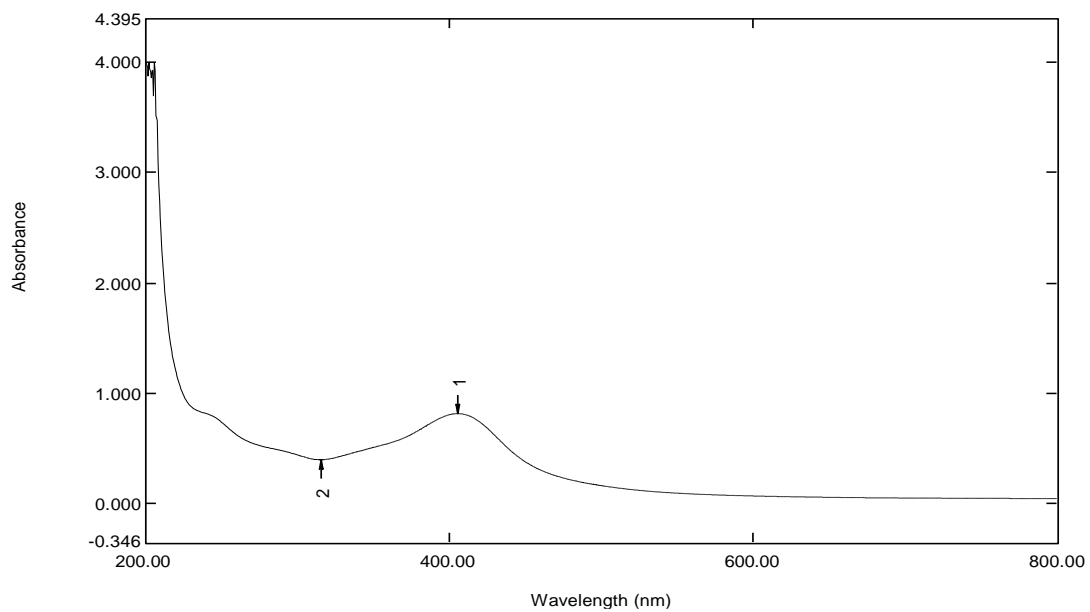Figure 4.3: UV- Visible Spectrum of Ethanol fraction mediated Silver Nanoparticles
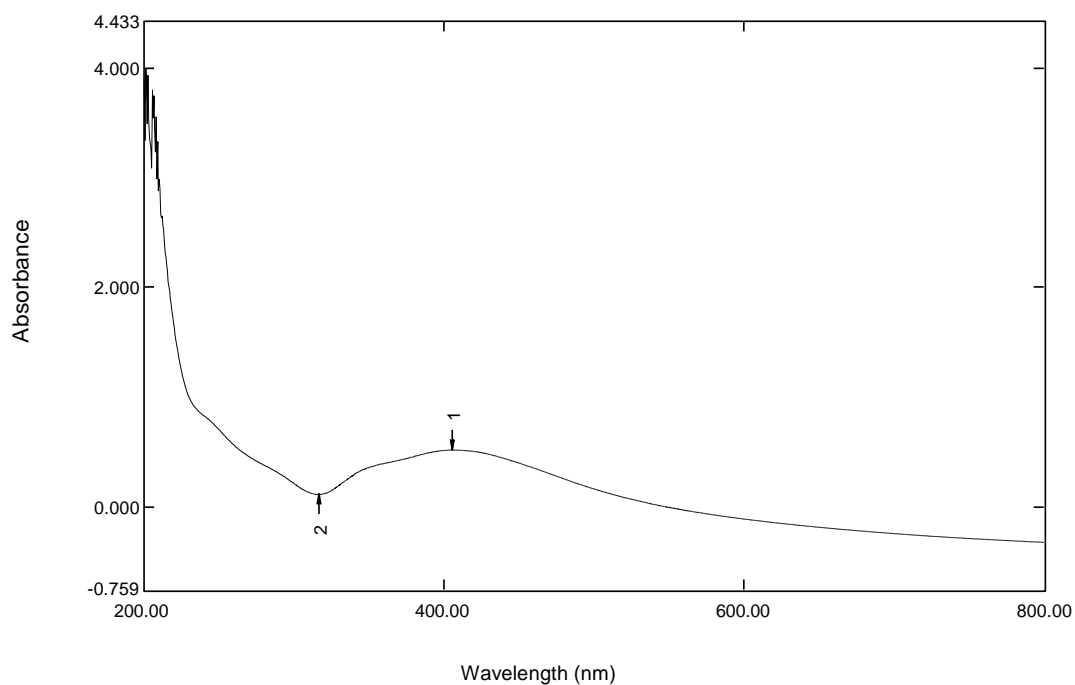
Figure 4.4: UV- Visible Spectrum of Chloroform fraction mediated Silver Nanoparticles

54
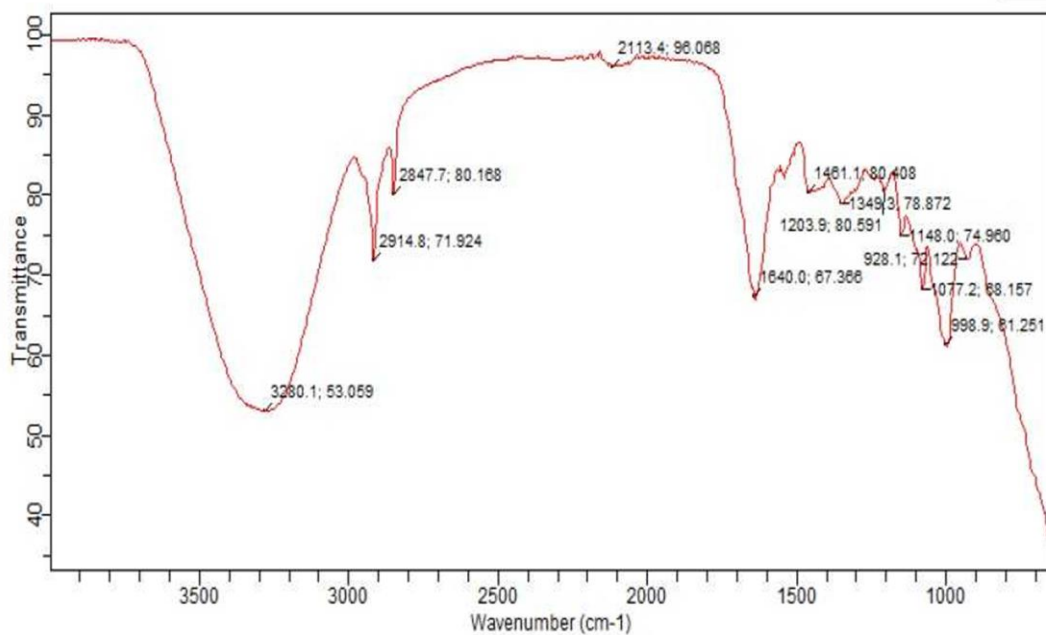
Figure 4.5: Fourier-transform Infrared Spectrum (FTIR) of Ethyl acetate fraction

mediated Silver Nanoparticles
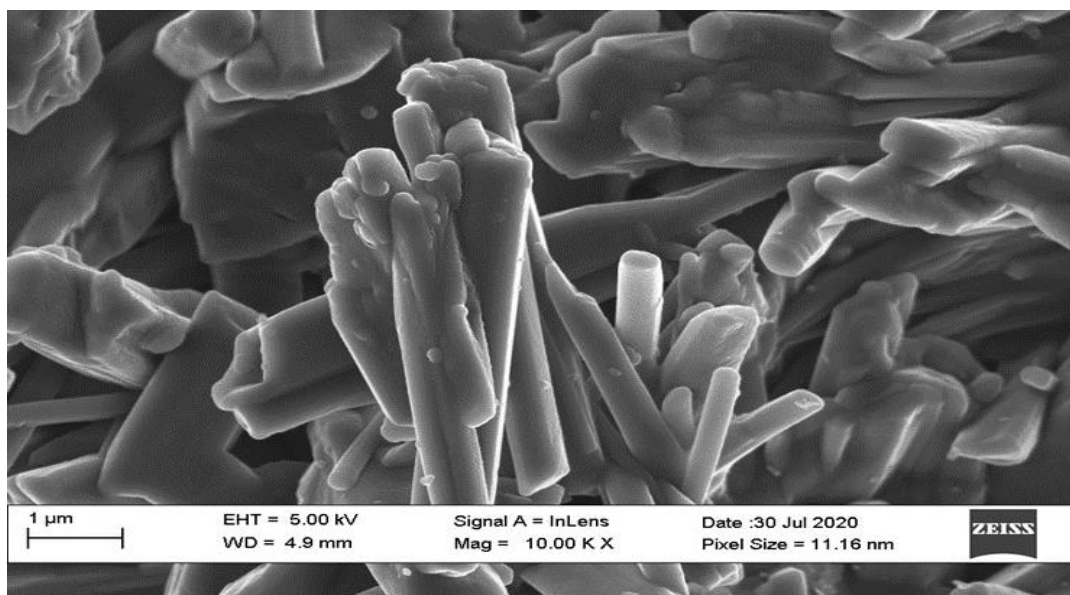
Figure 4.6: Scanning Electron Micrograph (SEM) of Ethyl acetate fraction mediated

Silver Nanoparticles.

Element	Atomic %
C	61.79
O	27.45
Na	9.05
Si	0.05
P	0.15
S	0.11
Cl	0.05
K	0.97
Ag	0.37
Total:	100

Figure 4.7: Energy Dispersive X-ray (EDX) of Ethyl acetate fraction mediated Silver

Nanoparticles

Figure 4.8: X- ray Diffraction (XRD) patterns of Ethyl acetate fraction mediated
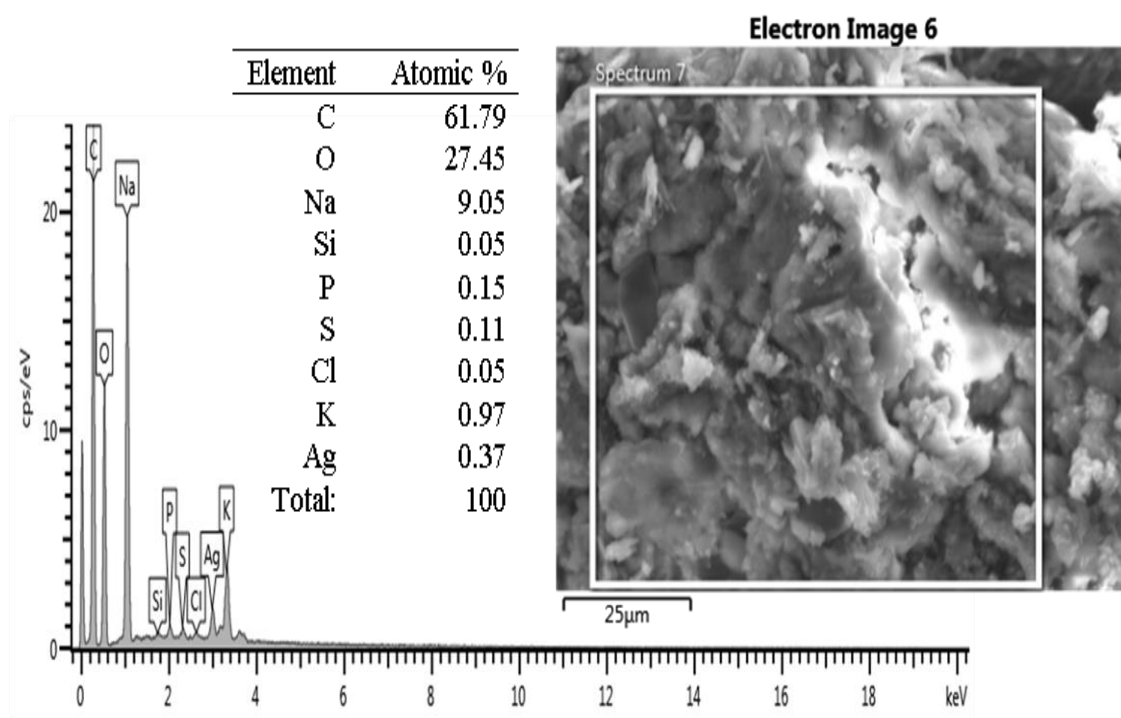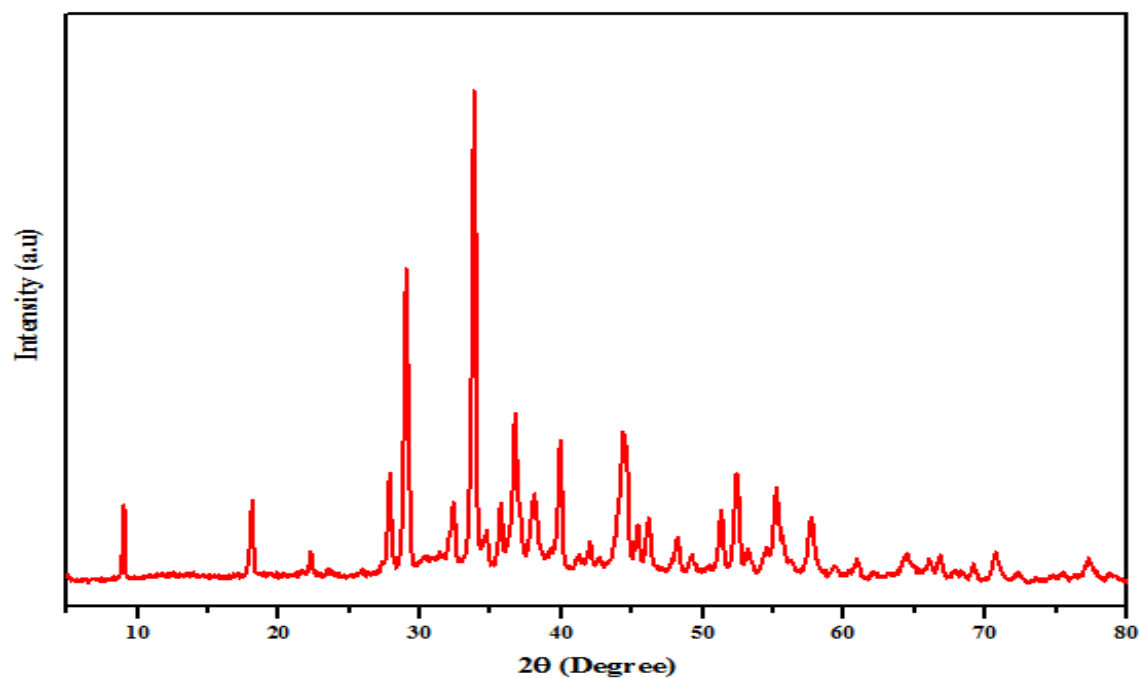
Silver Nanoparticles.

4.1.6 Antibacterial activities of *Curcuma longa* extract-mediated Silver Nanoparticle against Test Isolates.

The antibacterial activities of extract-mediated silver nanoparticles against test isolates at 2 mg content and 4 mg content are shown in Tables 4.7 and 4.8 respectively. The zones of inhibition produced by Eaq-AgNPs are 2.6 ± 0.6 mm, 6 ± 1.5 mm, 8 ± 0.5 mm and 10 ± 0.5 mm for *E. coli, K. pneumoniae, P. aeruginosa* and *S. pyogenes.* The E-AgNP produced zones of inhibitions of 5 ± 0.0 mm, 10 ± 0.5 mm and 12 ± 0.5 mm against *K. pneumoniae, S. pyogenes* and *P. aeruginosa* respectively while the zones of inhibition produced by Eea-AgNP was 7 ± 1.7 mm, 10 ± 0.7 mm, 11 ± 1.1 mm and 14 ± 0.5 mm against *S. pyogenes, P. aeruginosa, E. coli* and *K. pneumoniae.* The Ec-AgNPs produced zones of inhibition of 6 ± 1.5 mm, 8 ± 0.5 mm and 10 ± 0.5 mm against *P. aeruginosa, K. pneumoniae* and *E. coli.* The $AgNO_3$ produced zones of inhibition of 15 ± 1.7 mm, 16 ± 0.5 mm, 17 ± 1.7 mm, 17 ± 1.5 mm and 18 ± 0.0 mm for *S. pyogenes, S. aureus, E. coli, P. aeruginosa* and *K. pneumoniae* (Table 4.7). Table 4.8 shows the antibacterial activity of extracts mediated silver nanoparticle against test isolates at 400 mg/mL. The zones of inhibition produced by Eaq-AgNPs are 7 ± 1.7 mm and 10 ± 0.5 mm for *S. pyogenes* and *P. aeruginosa.* The E-AgNPs produced zones of inhibition of 5 ± 00 mm and 12 ± 0.5 mm against *P. aeruginosa* and *S. pyogenes* respectively while the zones of inhibition produced by Ec-AgNPs was 10 ± 0.5 mm against *S. pyogenes.* The $AgNO_3$ produced zones of inhibition of 15 ± 1.7 mm, 16 ± 0.5 mm, 17 ± 1.5 mm, 17 ± 1.7 mm and 18 ± 0.0 mm against *S. pyogenes, S. aureus, E. coli, P. aeruginosa* and *K. pneumoniae.*

Table 4.7: Antibacterial Activities of *Curcuma longa* extract/fractions-mediated Silver Nanoparticles at 2 mg Content

	Inhibition Zone Diameter (in mm) against Test Isolates				
NPS	*Pseudomonas aeruginosa*	*Escherichia coli*	*Klebsiella pneumoniae*	*Streptococcus Pyogenes*	*Staphylococcus aureus*
Eaq-AgNP	08.00 ± 0.5^a	02.60 ± 0.6^b	06.00 ± 1.5^{ab}	10.00 ± 0.5^b	00.00 ± 0.0^a
E-AgNP	12.00 ± 0.5^c	00.00 ± 0.0^a	05.00 ± 0.0^a	10.00 ± 0.5^b	00.00 ± 0.0^a
Eea-AgNP	10.00 ± 0.7^{bc}	11.00 ± 1.1^c	14.00 ± 0.5^c	07.00 ± 1.7^b	00.00 ± 0.0^a
Ec-AgNP	06.00 ± 1.5^a	10.00 ± 0.5^c	08.00 ± 0.5^b	00.00 ± 0.0^a	00.00 ± 0.0^a
AgNO$_3$	17 ± 1.7^d	17 ± 1.5^d	18 ± 0.0^d	15 ± 1.7^c	16 ± 0.5^b

Values are zone of inhibition mean ± standard error of mean of triplicate determination. Values with the same superscript letters in the same column are not significantly different at $P < 0.05$.

NPs: Nanoparticles

Eaq-AgNP: Aqueous fraction mediated silver nanoparticles   mg/mL: milligram per millilitre

E-AgNP: Ethanol extract mediated silver nanoparticles   mm: millimeter

Eea-AgNP: Ethyl acetate fraction mediated silver nanoparticles

Ec-AgNP: Chloroform fraction mediated silver nanoparticles

Table 4.8: Antibacterial Activities of *Curcuma longa* extract/fractions-mediated Silver Nanoparticles at 4 mg Content

NPs	Inhibition Zone Diameter (in mm) against Test Isolates				
	Pseudomonas aeruginosa	*Escherichia coli*	*Klebsiella pneumoniae*	*Streptococcus Pyogenes*	*Staphylococcus aureus*
Eaq-AgNP	10.00 ± 0.5^c	00.00 ± 0.0^a	00.00 ± 0.0^a	07.00 ± 1.7^b	00.00 ± 0.0^a
E-AgNP	05.00 ± 0.0^b	00.00 ± 0.0^a	00.00 ± 0.0^a	12.00 ± 0.5^{cd}	00.00 ± 0.0^a
Eea-AgNP	00.00 ± 0.0^a	00.00 ± 0.0^a	00.00 ± 0.0^a	00.00 ± 0.0^a	00.00 ± 0.0^a
Ec-AgNP	00.00 ± 0.0^a	00.00 ± 0.0^a	00.00 ± 0.0^a	10.00 ± 0.5^{bc}	00.00 ± 0.0^a
AgNO$_3$	17 ± 1.7^c	17 ± 1.5^b	18 ± 0.0^b	15 ± 1.7^d	16 ± 0.5^b

Results shows zone of inhibition size mean ± standard error of mean of triplicate determination. Values with the same superscript letters in the same column are not significantly different at $P < 0.05$.

NPs: Nanoparticles

Eaq-AgNP: Aqueous fraction mediated silver nanoparticles   mg/mL: milligram per millilitre

E-AgNP: Ethanol extract mediated silver nanoparticles   mm: millimeter

Eea-AgNP: Ethyl acetate fraction mediated silver nanoparticles

Ec-AgNP: Chloroform fraction mediated silver nanoparticles

4.1.7 Minimum Inhibitory Concentration of extract/fraction-mediated Silver Nanoparticles against Test Isolates.

The MIC of ethyl acetate fraction-mediated silver nanoparticle of *C. longa* against test isolates are shown in Table 4.9. The MIC of the extract against *P. aeruginosa, E. coli, K. pneumoniae* and *S. pyogenes* was at 12.5 mg/mL respectively.

The MIC of ethanol extract mediated silver nanoparticles of *C. longa* extract test isolates are shown in Table 4.9. The MIC of the extract against *K. pneumoniae, S. pyogenes* and *P. aeruginosa* was at 12.5 mg/mL and 25 mg/mL respectively while it was at 50 mg/mL for *Escherichia coli* respectively.

The MIC of aqueous fraction mediated silver nanoparticles of *C. longa* extract against test isolates are shown in Table 4.9. The MIC of the extract against *K. pneumoniae, S. pyogenes, E. coli* and *P. aeruginosa* was at 12.5 mg/mL and 25 mg/mL respectively.

Table 4.9 shows the MIC of chloroform fraction mediated silver nanoparticles of *Curcuma longa* extract on *K. pneumoniae, S. pyogenes, P. aeruginosa,* and *E. coli.* The MIC of the extract against *K. pneumoniae* and *P. aeruginosa* was at 25 mg/mL while for *S. pyogenes* and *E. coli* was at 12.5 mg/mL.

Table 4.9: Minimum Inhibitory Concentrations of extract/fraction-mediated Silver Nanoparticles against Test Isolates

Test Isolates	Minimum Inhibitory Concentration (mg/mL)			
	E-AgNP	Eaq-AgNP	Eea-AgNP	Ec-AgNP
Klebsiella pneumoniae	12.5	12.5	12.5	25.0
Streptococcus pyogenes	12.5	12.5	12.5	12.5
Pseudomonas aeruginosa	25.0	25.0	12.5	25.0
Escherichia coli	50.0	12.5	12.5	12.5

mg/ml = Milligram per Millilitre; NP = Nanoparticle; NP = Nanoparticle; E-AgNP = Ethanol extract-mediated Nanoparticle; Eaq-AgNP; Aqueous fraction-mediated Silver Nanoparticle; Eea-AgNP = Ethyl acetate fraction-mediated Silver Nanoparticle; Ec-AgNP = Chloroform fraction-mediated Silver Nanoparticle

4.1.8. Wound Healing Activity of Ethyl acetate fraction-mediated Silver Nanoparticles

Rat induced with 150 mg/kgbw of alloxan became diabetic after 3 days with blood sugar level ≥ 250 mg/dl. The diabetic rats were observed to be blind or having blurred vision, fatigued, they frequently urinated with reduced weight. The infected wound on the skin of the animals were observed to be inflamed, rapidly spreading, smelly liquid characterized by exudates. There was confluent growth on inoculated plate characterized by different colonies similar to those cultured from patients with diabetic foot infection. Yellow- green pigment, white greyish colour, clumps, mucoid large dome shape and greyish round-coloured colonies were observed. Gram staining characteristics was similar to *P. aeruginosa*, *S. pyogenes, S. aureus, K. pneumoniae* and *E. coli.*

The initial diameter of wound taken for all the nine groups were between the range of 1.23 ± 0.00 - 1.29 ± 0.19 mm (Table 4.10) subsequent treatment of the wound with the

ointment reduced the diameter of the wound from 0.3 ± 0.2 - 0.73 ± 0.00 mm. There was total wound closure after 14 days in all the treatment groups as compared to the negative control (Diabetes + wound only) 1.23 ± 0.00 to 1.1 ± 0.3 mm. There was significant ($P < 0.05$) wound closure observed from day 10 in all the treated groups (group 1-6) as compared to group 7 (Diabetes + Wound only) which has the highest wound size. Groups 8 (Wound only) and 9 (Wound + ointment) has the smallest size of wound when compared to the treated groups at day 10.

Table 4.10: Wound Healing Activity of Ethyl acetate fraction-mediated Silver Nanoparticles

GROUPS	Wound Diameter (mm) at various times							
	0	2	4	6	8	10	12	14
1	1.26 ± 0.0^a	1.35 ± 0.15^a	1.3 ± 0.0^a	1.24 ± 0.24^a	1.2 ± 0.2^a	1 ± 0.0^{bc}	0.8 ± 0.2^{ab}	0.62 ± 0.12^{ab}
2	1.29 ± 0.19^a	1.24 ± 0.0^a	1.2 ± 0.2^a	1.17 ± 0.0^a	1 ± 0.0^a	0.98 ± 0.02^{abc}	0.82 ± 0.02^{ab}	0.72 ± 0.2^{ab}
3	1.28 ± 0.08^a	1.257 ± 0.05^a	1.20 ± 0.0^a	1.01 ± 0.01^a	0.8 ± 0.3^a	0.81 ± 0.0^{abc}	0.8 ± 0.4^{ab}	0.73 ± 0.0^{ab}
4	1.27 ± 0.07^a	1.24 ± 0.24^a	1.19 ± 0.0^a	1.2 ± 0.2^a	0.7 ± 0.2^a	0.6 ± 0.3^{ab}	0.5 ± 0.0^a	0.4 ± 0.1^a
5	1.25 ± 0.0^a	1.22 ± 0.22^a	1.13 ± 0.03^a	1.07 ± 0.07^a	0.7 ± 0.3^a	0.66 ± 0.0^{ab}	0.57 ± 0.02^a	0.43 ± 0.03^a
6	1.24 ± 0.12^a	1.2 ± 0.0^a	1.11 ± 0.11^a	1.06 ± 0.0^a	0.92 ± 0.02^a	0.86 ± 0.05^{abc}	0.77 ± 0.0^{ab}	0.68 ± 0.08^{ab}
7	1.23 ± 0.00^a	1.23 ± 0.2^a	1.21 ± 0.3^a	1.21 ± 0.01^a	1.18 ± 0.1^a	1.15 ± 0.05^c	1.14 ± 0.0^b	1.1 ± 0.3^b
8	1.25 ± 0.25^a	1.05 ± 0.05^a	1 ± 0.0^a	0.92 ± 0.02^a	0.6 ± 0.3^a	0.53 ± 0.1^a	0.51 ± 0.11^a	0.46 ± 0.02^a
9	1.27 ± 0.0^a	1.10 ± 0.1^a	1.01 ± 0.11^a	0.95 ± 0.05^a	0.66 ± 0.0^a	0.53 ± 0.2^a	0.46 ± 0.0^a	0.3 ± 0.2^a

Values are wound closure mean ± standard error of mean of triplicate determinations. Values with the same superscript in the same column are not significantly different at $P < 0.05$.

Group1: Diabetes + Wound + *S. pyogenes* + Ointment, Group2: Diabetes + Wound + *E. coli* + Ointment, Group3: Diabetes + Wound+ *K. pneumoniae* + Ointment, Group4: Diabetes + Wound + *S. aureus* + Ointment, Group5: Diabetes + Wound + *P. aeruginosa* + Ointment, Group6: Diabetes + Wound + Mixed organisms + Ointment, Group7: Diabetes + Wound only (-ve control), Group8: Wound only (+ve control), Group9: Wound + Ointment, Group10: Shaved skin + Ointment.

4.1.8.1 *Histology of the Wounds*

Plates IV and V show the histology of skin of the control rats and those exposed to the Ethyl acetate - mediated silver nanoparticles for 14 days. The results obtained from the study revealed that the skin of groups 1 to 6 possessed fibroblast, collagens and inflammatory cells, groups 1, 3, and 5 had new blood vessels in their skin. Granulation tissues and blood capillaries were observed in groups 2, 5 and 6. Group 7 (negative control) possessed thinner epithelial layer with less and loosely packed collagen, fibroblast, blood vessels and high inflammatory cells. Group 8 (positive control) contained loosely packed collagen, fibroblast with irregular epithelialization and mild inflammatory cells. Complete epithelialization with regularly arranged collagen, more fibroblasts and blood vessels with less inflammatory cells were observed in group 9.

4.1.8.2 Safety of Ethyl acetate fraction-mediated Silver Nanoparticles

Treatment of rats in group 10 with Eea-AgNPs ointment was not accompanied with any adverse effect on the cells of the skin nor allergic reactions, rashes and other forms of skin irritation.
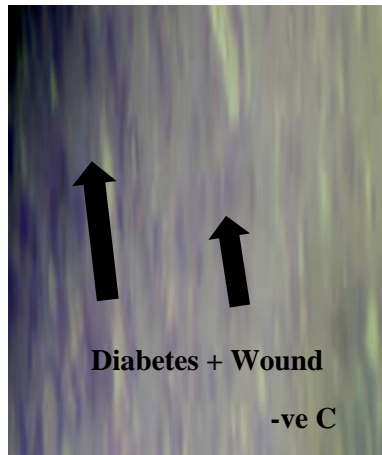
Diabetes + Wound -ve C

Wound only +ve C.

Wound + Extract only

Thinner epithelial layer with less and loosely packed collagen, fibroblast, blood vessels and high inflammatory cells.

Loosely packed collagen, fibroblast with irregular epithelialization and mild inflammatory cells.

Complete, epithelialization of the treated tissue with regularly arranged collagen, has more fibroblast and blood vessels with less inflammatory cells.

Diabetes + Wound + SP + Extract

Diabetes + Wound + EC + Extract

Diabetes + Wound + KP + Extract

Diabetes + Wound + SA + Extract

New blood-vessel formation with dense collagen deposition fibroblast and blood vessels with mild inflammatory cells.
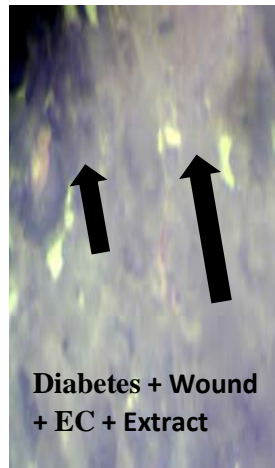
Granulation tissue contains mild collagen, fibroblast, blood capillaries, and mild inflammatory cells
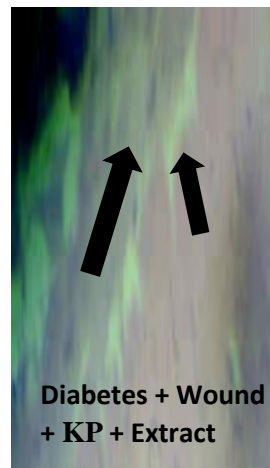
New blood-vessel formation with dense collagen deposition fibroblast and blood vessels with mild inflammatory cells.
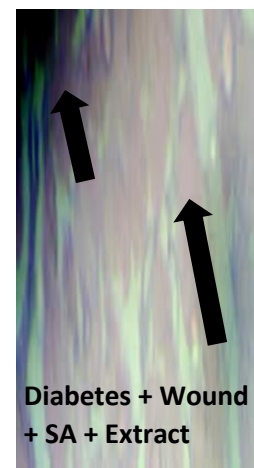
New blood-vessel formation with dense collagen deposition fibroblast and blood vessels with mild inflammatory cells.

SP: *Strep. pyogenes.*　　**EC**: *E. coli.*　**KC**: *K. pneumoniae.*　　**SA**: *Staph. aureus.*

Plate IV: Photomicrograph of the Skin Section of Rats Treated with *Curcuma longa* Extract Mediated Silver Nanoparticles
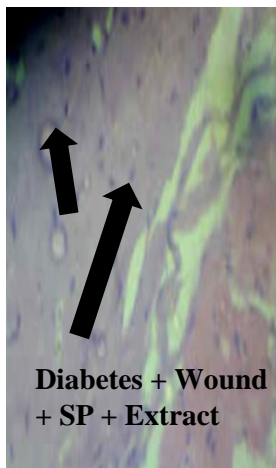
Diabetes + Wound -ve C

Thinner epithelial layer with less and loosely packed collagen, fibroblast, blood vessels and high inflammatory cells.

Wound only +ve C.

Loosely packed collagen, fibroblast with irregular epithelialization and mild inflammatory cells.

Wound + Extract only

Complete, epithelialization of the treated tissue with regularly arranged collagen, Has more fibroblast and blood vessels with less inflammatory cells.

Diabetes+ Wound + PA + Extract

Granulation tissue contains mild collagen, fibroblast, blood capillaries, and mild inflammatory cells.

Diabetes + Wound + Mixed + Extract

Granulation tissue contains mild collagen, fibroblast, blood capillaries, and mild inflammatory cells.

PA: *P. aeruginosa*.

Plate V: Photomicrograph of the Skin Section of Rats Treated with *Curcuma longa* Extract Mediated Silver Nanoparticles

4.2   Discussion

In the present study, the investigation revealed that most of the test organisms were oxidase negative (*S. pyogenes, K. pneumoniae, S. aureus* and *E. coli*), coagulase negative (*S. pyogenes, K. pneumoniae, P. aeruginosa* and *E. coli*), catalase positive (*K. pneumoniae, P. aeruginosa, S. aureus* and *E. coli*) (Table 4.4). This is similar with findings of Abdallah *et al. (*2018*)* and Alhubail *et al.* (2020) who identified similar organisms using this biochemical test. Gram staining of test isolate revealed Gram-positive cocci (*S. aureus* and *S. pyogenes*) and Gram-negative rods (*K. pneumoniae, P. aeruginosa* and *E. coli*). This is similar with the report of Abdallah *et al.* (2018) who used Gram staining to classify the same organisms.

In this study, it was observed that saponins, flavonoids, reducing sugar, steroids, tannins and anthraquinone were present in the crude extract and some portions of *C. longa* (Table 4.2). The results coincided with the findings of Okiki *et al.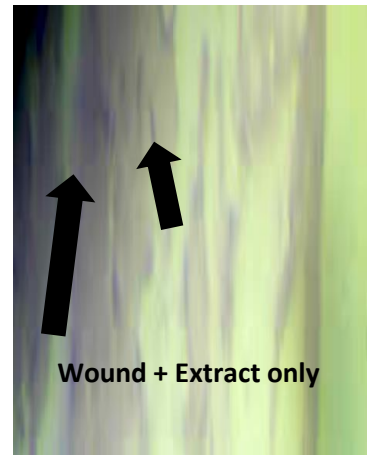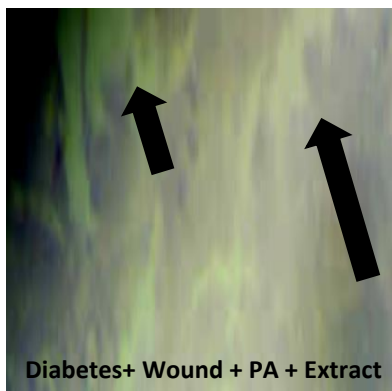*, (2017), Enemor *et al.*, (2020), and Muhammad and Fathuddin (2021) on *C. longa* containing the alkaloids, saponins, tannins, steroids, phenols, reducing sugars, cyanogenic glycoside and flavonoids.

In the present study, high concentration of phytate (6577.9 mg/100 g), cyanides (2741.8 mg/100 g) and saponins (618.0 mg/100 g) were observed in dried rhizomes of *C. longa*. This result contradicts the report of Okiki *et al.* (2017) that observed low level of phytate (45.0 mg/100 g) and saponins (420 mg/100 g). Phenols were present in the qualitative screening and absent in the quantitative screening of *C. longa*. This may be due to experimental error, specificity and sensitivity of the test. High phytate content significantly lowers cholesterol and risk of coronary diseases. Saponins and phytate helps in the management and prevention of diabetes as well as reducing growth of cancerous cells (Adeniyi *et al.,* 2016).

In this study, crude ethanol, ethyl acetate, chloroform and aqueous portions of *C. longa* at 1 mg content did not inhibit the growth of *P. aeruginosa, E. coli, K. pneumoniae, S. pyogenes* and *S. aureus* (Table 4.5). The inactivity of the extracts could be as a result of low concentration of antibacterial composition in the extract and extraction capacity of the solvent (Enemor *et al*., 2020).

The ethyl acetate portion (Eea) displayed marked antibacterial effect at 2 mg content against *P. aeruginosa, E. coli* and *S. pyogenes* (Table 4.6). The activity exhibited by the extract could be as a result of the high affinity of ethyl acetate solvent for the phytocomponents (reducing sugars, saponins and anthraquinone) Table 4.3. This result is similar with the findings of Ikpeama *et al.,* (2014) who screened ethanol, methanol and aqueous extracts of *C. longa* against similar organisms use in this study.

The formation of silver nanoparticles using rhizomes of *C. longa* crude extract ethanol (E) and fractions (Ethyl acetate, chloroform and aqueous) was viewed by colour change from yellow to dark brown. Similarly, Nadeem *et al.,* (2017) reported that the silver nanoparticles exhibited striking colour from yellow to brown. Silver nanoparticles exhibited yellowish brown colour in aqueous solution due to excitation of surface plasmon vibrations (Nadeem *et al*., 2017). By using UV- visible spectrum, the maximum absorbance peak for *C. longa* was seen at 405 nm, 406 nm, 409 nm and 410 nm for crude ethanol, chloroform, aqueous and ethyl acetate portions respectively. Similarly, Pirtarighat *et al.,* (2018) reported absorption spectra of silver nanoparticles formed in the reaction media have absorbance peak at 430 – 440 nm. Concentration and pH that had been identified as factors affecting the yields of silver nanoparticles were optimized. Fourier-transform infrared spectrum (FTIR) analysis (Figure 4.5) confirmed that the biomolecules of Ag^+ ions to silver nanoparticles is due to the reduction by capping

material of plant extract and revealed the presence of biomolecules that include aromatics, alkanes, alkenes, alkyls and carboxylic functional groups.

In the scanning electron microscope (SEM) micrograph (Figure 4.6), it was observed that rod like morphology and aggregated nanoparticles were in the size ranging from 11.16 nm – 40 nm with a variety of morphologies. Krithiga *et al*. (2015) also observed at 2Θ (8°, 18°, 27°, 29°, 34°, 37°, 40°, 45°, 53° and 57°) respectively which indicated the crystallinity of silver nanoparticles. This finding is similar to the observation by Swathi (2020) who reported strong diffraction peak of curcumin at 2Θ value of 19°, 38°, 25°, 50° and 45° respectively. The sharpness of the diffraction peaks indicated the crystalline nature of nanoparticles.

In this finding, energy dispersive analysis (EDX) spectrum exhibited signals of silver and other elements from the synthesised nanoparticles. The EDX spectrum indicated weak signals of silicon (Si), phosphorus (P), sulphur (S), silver (Ag) and potassium (K). This may be due to the biomolecules in the extract bound to the surface of biosynthesized AgNPs. However, the high presence of signal of C, O and Na may be due to environmental interferences during sample preparation on a glass substrate (Aamir *et al.,* 2015). This finding differs from the findings of Srirangam and Rao (2017), who reported high present of Ag with moderate amount of C, O and Cl. Silver nanoparticles obtained from *C. longa* Eea-AgNPs at 200 mg/mL had very strong inhibitory action against *Klebsiella pneumoniae, Escherichia coli* and *Pseudomonas aeruginosa* (Table 4.7). At 400mg/ml, Eea-AgNPs showed no inhibitory activity against any of the test organisms. The inhibitory effect demonstrated by Eea-AgNPs appeared to be dose independent on *P. aeruginosa, E. coli, K. pneumoniae* and *S. pyogenes.* The (E-AgNPs) displayed dose dependent antimicrobial effect on *Streptococcus pyogenes.* Krithiga *et al.,* (2015) observed that silver nanoparticles obtained from *Clitoria ternatea* and *Solanum nigrum*

have very strong inhibitory action against *Pseudomonas aeruginosa, Staphylococcus aureus, Escherichia coli* and *Streptococcus viridans.*

The AgNPs prepared from rhizomes of turmeric extract exhibited higher antibacterial activity than the crude extract and fractions. The enhancement of the activity is most likely based on the silver particles released by AgNPs that are capable of destroying cell walls and secondary metabolites adsorbed on AgNPs with easier penetration into the cells (Elemike *et al.,* 2017; Salayova *et al.,* 2021). Also, bioactive compounds could be responsible for the increased antibacterial activity of Eea-AgNPs and improved ability to interact with the cell wall.

In this study, 150 mg/kgbw of alloxan were administered to rats (Groups 1 to 7) via intraperitoneal route similar method was carried out by Oluwafemi *et al.,* (2017). Animals having blood glucose level $\geq$ 250 mg/dl on the third day after alloxan injection were considered diabetic. In the present research, wound inoculated with test isolates showed symptoms such as swollen, smelly liquid draining from the wound and infiltration of wound, Wubante *et al.* (2018) made similar observations in infected wound models treated with crude extract of *Akanthus polystachyus* leaf.

In the present study, significant difference ($P > 0.05$) was observed in wound closure from Day 10 – 14 in all the treated groups (Groups 1 - 6) (Table 4.10) due to the ability of Eea-AgNPs to enhance collagen synthesis, new blood vessel formation and antimicrobial effect of bioactive components. Wubante *et al.* (2018) made similar observations on the ability of *Acanthus polystachyus* leaf extract to enhance collagen formation, induction of cell proliferation and antimicrobial activities. Epithelialization is essential for wound healing (Paul *et al*., 2017; Berbudi *et al*., 2021). Venkatasubbu and Anusuya (2017) reported that *C. longa* caused enhanced formation of granulation tissue, deposition of collagen, remodeling of tissue and contraction of wound in rats.

In vivo antimicrobial and the ointment of Eea-AgNPs showed remarkable wound healing ability in rats infected with test isolates (*P. aeruginosa, K. pneumoniae, S. pyogenes, E. coli and S. aureous*). The infiltration, blister formation, swollen and exudates exhibited in wounds of rats before treatment vanished in all the treated groups (1 - 6) except group 7 (Diabetes + wound). Groups treated with extract showed faster rate of wound contractions than group 7, this revealed the wound healing ability of Eea-AgNPs and this is similar with the findings of Mills *et al.* (2019).

In the present investigation, the antibacterial activity of the Eea-AgNPs was confirmed against wound infecting pathogens which indicated its remarkable fast healing rate. The eradication of the colonizing organisms from the infected wounds created a suitable environment for wound healing to occur. Thus, the antimicrobial activity showed by the Eea-AgNPs in infected wound model revealed the promising potentials of *C. longa* in the management of wounds. This result is further strengthened by the *in vitro* antibacterial activity against test isolates. The presence of phytochemicals (flavonoids, phenols, steroids, saponins and tannins) in crude extract of *C. longa* could singly or synergistically contribute to its wound healing activity Wubante *et al.* (2018) made similar observations in *Acanthus polystachyus* and concluded that the plant phytoconstituents may be responsible for the remarkable wound healing capabilities.

The absence of mortality and toxicity (lack of allergic reaction, irritations and rashes) indicated that Eea-AgNPs is relatively nontoxic and safe for topical application.

CHAPTER FIVE

5.0   **CONCLUSION AND RECOMMENDATIONS**

5.1   **Conclusion**

Phytochemical constituents such as flavonoids, reducing sugar, tannins, anthraquinone and phytates were present in the crude extract and fractions of *C. longa*. Very high quantities of phytates (6577.9 mg/100 g), cyanides (2741.8 mg/100 g) and saponins (618.0 mg/100 g) were dictated in *C. longa* powder. The results of the study revealed that crude ethanol, ethyl acetate, chloroform and aqueous portions of *C. longa* at 1 mg content did not inhibit the growth of *P. aeruginosa, E. coli, K. pneumoniae, S. pyogenes* and *S. aureus*. The crude ethyl acetate portion at 2 mg content however inhibited the growth of *P. aeruginosa, E. coli* and *S. pyogenes*. The Eea-AgNPs displayed dose independent marked inhibiting effect against *K. pneumoniae, E. coli* and *P. aeruginosa*.

The MIC of Eea-AgNPs of *C. longa* against *P. aeruginosa, E. coli, K. pneumoniae* and *S. pyogenes* was at 12.5 mg/mL each. The extracts showed bacteriostatic effect against the test organisms.

Silver nanoparticles using rhizomes of *C. longa* crude extract (E) and fractions (Eea, Ec and Eaq) was formed by colour change from yellow to dark brown. The maximum absorbance was at 405 nm, 406 nm, 409 nm and 410 nm for crude ethanol, chloroform, ethyl acetate and aqueous fractions respectively. The FTIR analysis indicate the presence of biomolecules that includes aromatic, alkanes, alkynes, alkenes, alkyls and carboxylic functional groups. The SEM micrograph of EeaAgNPs revealed rod like morphology and aggregated nanoparticles while its XRD peaks were observed at 2Θ (8°, 18°, 27°, 29°, 34°, 37°, 40°, 45°, 53 and 57°).

The extract displayed significant ($P < 0.05$) wound healing activity from day 10 – 14 in diabetic rats and normal rats.

The EaAgNPs is relatively safe for topical application in experimental rats.

5.2   Recommendations

i. This investigation contributes to the knowledge of antibacterial efficacy of *C. longa* and validate the traditional claims of the medicinal plant for treatment of infection.

ii. Eea-AgNPs is topically safe and should be considered as a natural source of antibacterial for the treatment and management of diabetic foot infection.

iii. Further research is required to explore the mode of action of the medicinal plant on the pathogens.

REFERENCES

Aamir, I. W., Veluswamy, P., Anusya, T., Kamran, M. W., & Shah, A. H. (2015). Synthesis and characterization of Silver Nano rod like Structures by Green Synthesis method using *Curcumin Longa. International Journal of ChemTech Research*, 7(3), 1504-1508.

Abdallah, M. S., Mustapha, T., Gambo, A., & Ishaq, S. (2018). Biochemical Identification and Cultural Characterization of Some Gram- Negative Bacteria Obtained From Fecal /Diarrhoeal Samples. *CIBTech Journal of Microbiology*, *5*(1), 31–34.

Abdissa, D., Adugna, T., Gerema, U., & Dereje, D. (2020). Prevalence of Diabetic Foot Ulcer and Associated Factors among Adult Diabetic Patients on Follow-Up Clinic at Jimma Medical Center, Southwest Ethiopia, 2019: An Institutional-Based Cross -Sectional Study. *Journal of Diabetes Research*, 10, 1-6.

Abolghasemi, V., & Mesri, M. (2019). Update on New Therapies of Diabetic Foot Ulcers: A Systematic Review. *Journal of International Translational Medicine*, 7(1), 61-64.

Adeniyi, K. A., Olayemi, I. K., Shittu, K. O., Busari, M. B., Mohammed, S., Bashir, L., & Yusuf, R. S. (2016). Comparative phytochemical and antinutritional constituents of Nigeria sweet and bitter honey varieties. *World Journal of Pharmaceutical Research*, 5(3), 255-267.

Ahmad, S., Munir, S., Zeb, N., Asad, U., Khan, B., Ali, J., Muhammad, B., Muhammad, O., Muhammad, A., Syed, M. S., & Saqib, A. (2019). Green nanotechnology: a review on green synthesis of silver nanoparticles - an ecofriendly approach. *International Journal of Nanomedicine,* 14, 5087–5107.

Ahmad, W., Saqibah, R., Amna, K., Dastageer, W., & Saima, B. (2020). Pattern of Bacteriological Culture and Antimicrobial Sensitivity in Diabetic Foot Ulcer: A Cohort Study from District Dera Ismail Khan. *Multidisciplinary European Academic Journal*, 2(1), 1-7.

Alhubail, A., Sewify, M., Messenger, G., Masoetsa, R., Hussain, I., Nair, S., & Tiss, A. (2020). Microbiological profile of diabetic foot ulcers in Kuwait. *PLoS ONE*, *15*(12), 1–15.

Alsammarraie, F. K., Wang, W., Zhou, P., Mustapha, A., & Lin, M. (2020). Green Synthesis of Silver Nanoparticles Using Turmeric Extracts and Investigation of their Antibacterial Activities. *Colloids and Surfaces B: Biointerfaces,* 10, 1-29.

Alvarado-Gomez, E., Perez-Diaz, M., Valdez-Perez, D., Ruiz-Garcia, J., & Magana-Aquino, M. (2017). Adhesion forces of biofilms developed *in vitro* from clinical strains of skin wounds. *Material Science Engineering,* 82, 336-344.

Ambrose, A**.**, & Christopher, L. (2019). Prevalence and Determinants of Diabetic Foot Ulcers and Lower Extremity Amputations in Three Selected Tertiary Hospitals in Ghana. *Journal of Diabetes Research,* 10, 1-9.

Babayi, H., Alabi, R. O., Amali, E. D., & Baba, E. (2018). Effects of Oral Administration of Aqueous Extract of Tridax procumbens Leaves on Some Haematological Variables in Rats. *Modern Chemistry & Applications*, 6(1), 1-5.

Bahar, M., Ashebr, A., Teka, F., Adugna, N., & Solomon, A. (2018). *In-vitro* antibacterial activity of selected medicinal plants in traditional treatment of skin and wound infections in eastern Ethiopia.

Baran, M. F., & Acay, H. (2019). Antimicrobial Activity of Silver Nanoparticles Synthesized with Extract of Tomato plant Against Bacterial and Fungal Pathogens. *Middle Black Sea Journal of Health Science,* 5(2): 67-73.

Begum, K., Mannan, S. J., Rezwan, R., Rahman, M. M., Rahman, M. S., & Nur-E-Kamal, A. (2017). Isolation and characterization of bacteria with biochemical and pharmacological importance from soil samples of Dhaka city. *Dhaka University Journal of Pharmaceutical Sciences*, *16*(1), 129–136.

Bello, S., Mohammed, B., & Muhammad, Y. (2018). Survey of Bacteria and Fungi Associated with Suspected Cases of Meningitis Among Children Attending Some Selected Hospitals in Kano. *Bayero Journal of Pure and Applied Sciences,* 11(2), 279-285.

Berbudi, A., Anshori, H., Andromeda, A., Kwarteng, A., Putri, A. C., & Atik, N. (2021). Topical administration of *Curcuma longa L.* extract gel increases M2 macrophage polarization and collagen density in skin excision. *Journal of Applied Pharmacuetical Science,* 11(1), 95-100.

Bitrus, A. A., Olabode, M. P., Muhammad, A. A., & Mohammed, D. G. (2018). *Staphylococcus aureus*: A Review of Antimicrobial Resistance Mechanisms. *Veterinary Sciences: Research and Reviews,* 4(2), 43-54.

Boulton, A. J. M., David, G. A., Robert, S. K., Christopher, E. A., Lawrence, A. L., Benjamin, A. L., Joseph, L., & Mills, J. S. (2018). Steinberg. Diagnosis and Management of Diabetic Foot Complications. *American Diabetes Association,* 6, 1-20.

Bshabshe, A., Martin, R. P. J., Amgad, A. A., Abdalla, N. F., Harish, C. C., & Mohamed, E. H. (2020). Clinical Relevance and Antimicrobial Profiling of Methicillin-Resistant *Staphylococcus aureus* (MRSA) on Routine Antibiotics and Ethanol Extract of Mango Kernel (*Mangifera indica* L.). *Biomedical Research International,* 1, 1-8.

Chanda, S., & Ramachandra, T. V. (2019). Phytochemical and Pharmacological Importance of Turmeric (*Curcuma longa*): A Review. *Research & Reviews: A Journal of Pharmacology,* 9(1), 16-23.

Chao, C., Chun-Ming, W., Shao-Ping, L., Li-Gen, L., Wen-Cai, Y., & Qing-Wen, Z. (2018). Simultaneous Quantification of Three Curcuminoids and Three Volatile Components of Curcuma longa Using Pressurized Liquid Extraction and High-Performance Liquid Chromatography. *Molecules*, 23, 1-9.

Choudhury, D. (2019). Study on the nutrient composition of local variety of turmeric (*Curcuma longa*). *The Pharma Innovation Journal,* 8(2), 205-207.

DanMusa, U. M., Lorliam, T., Idris, A. N., Auwal, A. A., & Yahya, H. M. (2016). Prevalence and healthcare cost associated with the management of diabetic foot ulcer in patients attending Ahmadu Bello University Teaching Hospital Nigeria. *International Journal of Health Sciences,* 10(2), 219-228.

Davarci, I., Senbaryrak, S., Aksaray, S., Kocoglu, M. E., Kuskucu, M. A., & Samasti, M. (2019). Molecular Epidemiology of Carbapenem-resistant *Klebsiella pneumoniae* Isolates. *Anadolu Klinigi*, 2(4), 1-7.

Diggle, S. P., & Whiteley, M. (2020). Microbe Profile: *Pseudomonas aeruginosa*: opportunistic pathogen and lab rat. *Microbiology,* 166, 30–33.

Divakaran, M., Dinsy, M. P., Poulose, C., Anjali, T., Anu, P. J., Anupama, V. C., & Latha, P. (2018). Studies on Morphology and Medicinal Efficacy of Nanoparticles Synthesized from Two Medicinally Important *Curcuma* Spp., *C. Longa* and *C. Caesia. International Journal of Advanced Research,* 6(9), 603-609.

Dons, T., & Soosairaj, S. (2018). Evaluation of wound healing effect of herbal lotion in albino rats and its antibacterial activities. *Clinical Phyto science*, 4(6), 1–7.

Egas, A. L., Martnez- Navarrete, N., & Camacho, M. (2020). Impact of biopolymers added to a grapefruit puree and freeze-drying shelf-life temperature on process time reduction and product quality. *Food and Bioproducts Processing.* 120, 243-150.

Elemike, E. E., Onwudiwe, D. C., Ekennia, A. C., & Katata-Seru, L. (2017). Biosynthesis, characterization, and antimicrobial effect of silver nanoparticles obtained using Lavandula. *Intermediate Journal of Research Chemistry*, 43, 1383–1394.

Enemor, V. H. A., Ogbodo, U. C., Nworji, O. F., Ezeigwe, O. C., Okpala, C. O., & Iheonunekwu, G. C. (2020). Evaluation of the Nutritional Status and Phytomedicinal Properties of Dried Rhizomes of Turmeric (*Curcuma longa*). *Journal of Biosciences and Medicines*, 8, 163-179.

Freschi, L., Vincent, A. T., Jeukens, J., Emond-Rheault, J. G., & Kukavica-Ibrulj, I. (2019). The *Pseudomonas aeruginosa* Pan-Genome provides new insights on its population structure, horizontal gene transfer, and pathogenicity. *Genome Biological Evolution,* 11, 109–120.

Garg, S., & Garg, A. (2018). Encapsulation of Curcumin in Silver Nanoparticle For Enhancement of Anticancer Drug Delivery *International Journal of Pharmaceutical Sciences and Research*, 9(3), 1160-1166.

Geographical Information System Achievers., (2021). Spatial Distribution of features in General Hospital Minna, *Study Area Map*, http: gisachievers.com

Gunasekaran. P. (2017). Assessment of major microorganisms involved in diabetic foot infection which delays wound healing. *International Archives of Integrated Medicine*. 4(8), 87-90.

Hassan, I., Bream, A. S., El-Sayed, A., & Yousef, A. M. (2017). Assessment of disinfection by-products levels in Aga surface water plant and its distribution system, Dakhlia, Egypt. *International Journal of Advance Research in Biological Sciences*, *4*(4), 37-43.

Hernandez, C. A., Juarez-Moreno, K., Martin, E. C., Almanza-Reyes, H., Alexey, P., & Bogdanchikova, N. (2017). Silver Nanoparticles for the Rapid Healing of Diabetic Foot Ulcers. *International Journal of Medical Nano Research,* 4(1), 1-6.

Ibrahim, A. M. (2018). Diabetic Foot Ulcer: Synopsis of the Epidemiology and Pathophysiology. *International Journal of Diabetes and Endocrinology*, 3(2), 23-28.

Iftikhar, A., Aslam, B., Iftikhar, M., Majeed, W., Batool, M., Zahoor, B., Amna, N., Gohar, H., & Latif, I. (2020). Effect of Caesalpinia bonduc Polyphenol Extract on Alloxan-Induced Diabetic Rats in Attenuating Hyperglycemia by Upregulating Insulin Secretion and Inhibiting JNK Signaling Pathway. *Oxidative Medicine and Cellular Longevity*, 1-16.

Ikpeama, A., Onwuka, G. I., & Nwankwo, C. (2014). Nutritional composition of tumeric (*Curcuma longa*) and its antimicrobial properties. *International Journal of Scientific & Engineering Research*, *5*(10), 1085–1089.

Karlsson, C. A. Q., Sofia, J., Lena, W., Christian, K., Lars, B., Adam, L., & Johan A. M. (2018). *Streptococcus pyogenes* infection and the human proteome with a special focus on the IgG-cleaving enzyme IdeS. *MCP Papers in Press,* 1-32.

Krebs-Holms, L. (2020). Turmeric: Nutritional value health benefits, storage and recipes. *eMediHealth*, 1-10.

Krithiga, N., Rajalakshmi, A., & Jayachitra, A. (2015). Green Synthesis of Silver Nano particles Using Leaf Extracts of *Clitoria ternatea* and *Solanum nigrum* and Study of Its Antibacterial Effect against Common Nosocomial Pathogens. *Journal of Nanoscience*, 1–8.

Laabei, M., & Ermert, D. (2019). Catch Me if You Can: *Streptococcus pyogenes* Complement Evasion Strategies. *Journal of Innate Immunity*, 11, 3–12.

Manandhar, S., Luitel, S., & Dahal, R. K. (2019). *In Vitro* Antimicrobial Activity of Some Medicinal Plants against Human Pathogenic Bacteria. *Journal of Tropical Medicine*. 1-5.

Makvana, S., & Krilov, L. (2015). Escherichia coli Infections. *Pediatrics in Review,* 36 (4), 167-171.

Mairghani, M., Elmusharaf, K., Patton, D., Eltahir, O., Jassim, G., & Moore, Z. (2017). The prevalence and incidence of diabetic foot ulcer among five countries in the Arab World: A systematic review. *Journal of wound Care*, 26(9), 27-24.

Mills, J. P., Payal, P., Burdick, S., DeGeorge, C., Gallagher, K. A., Holmes, M., Jacobson, J. A., Nagel, J. L., & David M. S. (2019). Diabetic Foot Infections. *Michigan Medicine*, 1-12.

Muhammad, F. M., & Fathuddin, R. (2021). The Screening for the Antitrypanosomal Potentials of the Extracts of *Curcuma longa L. Acta Scientific Microbiology*, *4*(2), 76–81.

Nadeem, M., Abbasi, B. H., Younas, M., Ahmad, W., & Khan, T. (2017). A review of the green syntheses and anti-microbial applications of gold nanoparticles. *Green* Chemistry *Letters and Reviews.* 10, 216–227.

Nauru Idalia, V., & Franco, B. (2017). *Escherichia coli* as a Model Organism and Its Application in Biotechnology. Recent Advances in Physiology, Pathogenesis and Biotechnological Applications, 253-274.

Netten, J. J., Bus, S. A., Apelqvist, J., Lipsky, B. A., Hinchliffe, R. J., Game, F., Rayman, G., & Schaper, N. C. (2019). Definitions and criteria for diabetic foot disease. *The Lancet Diabetes and Endocrinology*,1, 1–15.

Nicholas, D. B., Marion, C. D., Brian, K., Helen, E. H., Claire, M., Matthew, J. Y., Hannah M. A., Duncan, S., Stephanie, J. D., Andrew, S., & Graham, P. L. (2017). Diabetic foot infection: Antibiotic therapy and good practice recommendations. *International Journal of Clinical Practice*, 71, 1-10.

Oghenejobo, M., Opajobi, O. A., Bethel, O. U. S., & Uzoegbu, U. (2017). Antibacterial Evaluation, Phytochemical Screening and Ascorbic Acid Assay of Turmeric (*Curcuma longa*). *MOJ Bioequivalence & Bioavailability*, 4(2), 1-8.

Okiki, P. A., Borke, R. V., Odesanya, B. O., Muhammad, A. A., & Sobajo, O. A. (2017). Chemical Qualities of Dried Rhizomes of *Curcuma longa Linn.* and the Antimicrobial Activities of its Extracts on Microorganisms Associated in Skin Infections. *Der Pharma Chemica,* 9(21), 17–28.

Oluwafemi, A. G., Oseni, O. A., Ajayi, O. B., & Akomolafe, S. F. (2017). Inhibition of Alloxan-Induced Diabetes by Turmeric Pre-Treatment in Rats: The Effect on Antioxidant Enzymes in Some Organs (Liver, Kidney and Heart). *International Journal of Research in Pharmacy and Biosciences*, 4(6), 10-17.

Omeje, M., & Kelechi, N. (2019). In Vitro Study on the Antimicrobial Activity of *Curcuma longa* Rhizome on Some Microorganism. *American Journal of Biomedical and Life Sciences*, 7(1), 1-5.

Paczosa, M. K., & Mecsas, J. (2016). *Klebsiella pneumoniae*: Going on the Offense with a Strong Defense. *Microbiology and Molecular Biology Reviews,* 80(3), 629-650.

Patil, S. S., Pathak, A., & Rathod, V. K. (2021). Optimization and kinetic study of ultrasound assisted deep eutectic solvent based extraction : A greener route for extraction of curcuminoids from *Curcuma longa*. *Ultrasonics - Sonochemistry*, *70*, 1- 10.

Paul, S., Abu-Nasar, M. d., Rahman, A., Abdullah, A., Mahmud, A. U., & Ziban, C. D. (2017). Wound healing by marigold (*Calendula officinalis*) and turmeric (*Curcuma longa*) paste: A comparative approach. *Journal of Advanced Veterinary and Animal Research*, 4(4), 333-342.

Pirtarighat, S., Ghannadnia, M., & Baghshahi, S. (2018). Green synthesis of silver nanoparticles using the plant extract of *Saliva spinosa* grown *in vitro* and their antibacterial activity assessment. Journal of Nanostructure in Chemistry. 9, 1-9.

Poulsen, B. E., Yang R, Clatworthy, A. E., White, T., & Osmulski S. J. (2019). Defining the core essential genome of *Pseudomonas aeruginosa*. *Proceedings of National Academic of Science USA, Pp. 2-8.*

Public Health England. (2015). UK Standards for Microbiology Investigations: Staining Procedures. *Bacteriology*, (2)1, 1-52.

Rajsekhar, P. B., Bharani, R. S., K., Angel, K. J., Maya, R., & Sharadha, P. V. (2015). Curcumin Nanoparticles: A Therapeutic Review. *Research Journal of* Pharmaceutical*, Biological and Chemical Sciences,* 6(5), 1180-1185.

Ramirez-Acuna, J. M., Idalia, G., Sergio, A. C., Pedro, A. M., Flores-Morales, V., Perez-Favila, A., Miguel, A. C., & Martinez-Fierro, A. C. (2019). Diabetic Foot Ulcers: Current Advances in Antimicrobial Therapies and Emerging Treatments. *Antibiotics*, 8(193), 1-32.

Rashid, K., Chowdhury, S., Ghosh, S., & Sil, P. C. (2017). Curcumin attenuates oxidative stress induced NFkB mediated inflammation and endoplasmic reticulum dependent apoptosis of splenocytes in diabetes. *Biochemical Pharmacology*. 1, 140-155.

Rathore, S., Mukim, M., Sharma, P., Devi, S., Chandra Nagar, J., & Khalid, M. (2020). Curcumin: A Review for Health Benefits Kingdom of Saudi Arabia. *International Journal of Research and Review,* 7(1), 1-10.

Rave, A. F. G., Kuss, A. V., Peil, G. H. S., Ladeira, J. P. V., Villarreal, J. P. V., & Nascente, P. S. (2019). Biochemical Identification Techniques and Antibiotic susceptibility Profile of Lipolytic ambiental bacteria from effluents. *Brazilian Journal of Biology*. 79(4), 555-565.

Reyes, J., Aguilar, A. C., & Andres, C. (2019). Carbapenem-Resistant *Klebsiella pneumoniae*: Microbiology Key Points for Clinical Practice. *International Journal of General Medicine*, 12, 437–446.

Rivera-Mancia, S., Joyce, T., & Jose, P. C. (2018). Utility of *Curcumin* for the treatment of diabetes mellitus: Evidence from preclinical and clinical studies. *Journal of Nutrition and Intermediary Metabolism,* 14, 29-41.

Roshan, P. Y., & Gaur, T. (2017). Versatility of turmeric: A review the golden spice of life. *Journal of Pharmacognosy and Phytochemistry*, 6(1), 41-46.

Salayova, A., Zdenka, B., Daneu, N., Matej, B., Zdenka, L. B., Balazova, L., & Tkacikova, L. (2021). Green Synthesis of Silver Nanoparticles with Antibacterial Activity Using Various Medicinal Plant Extracts: Morphology and Antibacterial Efficacy. *Nanomaterials*, 11(1005), 1-20.

Salomoni, R., Leo, P., Montemor, A. F., Rinaldi, B. G., & Rodrigues, M. F. A. (2017). Antibacterial effect of silver nanoparticles in *Pseudomonas aeruginosa. Nanotechnology Science and Applications,* 10, 115–121.

Salutini, E., Brocco, E., Da-Ros, R., Monge, L., Uccioli, L., & Anichini, R. (2020). The Complexity of Diabetic Foot Management: From Common Care to Best Practice. The Italian Expert Opinion by Delphi Survey. *International Journal of Lower Extremity Wounds*, *19*(1), 34–43.

Sankar, R., Rahman, P. K., Anusha, C., Varunkumar, K., Kalaiarasi, A., Shivashangari, K. S., & Ravikumar, V. (2017). Facile synthesis of Curcuma longa tuber powder engineered metal nanoparticles for bioimaging applications. *Journal of Molecular Structure,* 1129, 8 -16.

Sawant, R. S., & Godghate, A. G. (2020). Qualitative Phytochemical Screening of Rhizomes of *Curcuma longa Linn. International Journal of Science, Environment and Technology*, 2(4), 634 – 641.

Shafaghat, A. (2015). Synthesis and characterization of silver nanoparticles by phytosynthesis method and their biological activity. *Synthesis and Reactivity in Inorganic, Metal-Organic and Nano-Metal Chemistry*, *45*(3), 381–387.

Sharifi-Rad, J., Youssef, E. l., Rayess, R. Z., Alain, A. R., Carmen, S., Katarzyna, N., Wissam, Z., Simona, S., Noura, S. D., Dorota, Z., Bahare, S., William, N. S., Yasaman, T., Marc, E. l., Miquel, M., Elise, A. O., Hafiz, A., William, C. C., Alfred, M., & Martins, N. (2020). Turmeric and Its Major Compound Curcumin on Health: Bioactive Effects and Safety Profiles for Food, Pharmaceutical, Biotechnological and Medicinal Applications. *Frontiers in Pharmacology*, 11(01021), 1-23.

Sharma, A., Khanna, S., Kaur, G., & Singh, I. (2021). Medicinal plants and their components for wound healing applications. *Future Journal of Pharmaceutical Sciences*, *7*(53), 1-13.

Sindhu, S. (2018). An Overview on Diabetic Foot Ulcer (DFU): Mini Review. *Diabetes Case Reports*, 3(1), 1-3.

Sin-Yeang, T., Kitson, L., Syed, A. A., Alan, S. K., & Suat-Cheng, P. (2016). Anti
bacterial Action of Curcumin against *Staphylococcus aureus*: A Brief Review.
Journal of Tropical Medicine. 10, 1-10.

Smith-Strom, H., Iversen, M. M., & Igland, J. (2017). Severity and duration of diabetic
foot ulcer (DFU) before seeking care as predictors of healing time: A retrospective
cohort study. *PLoS One*. 12(5), 177-179.

Srirangam, G. M., & Rao, K. P. (2017). Synthesis and characterization of silver Nano
particles from the leaf extract of *Malachra capitate (L.)*. *Journal of Chemistry*,
10(1), 46- 53.

Swathi, G., Reddy, G. R., Rajesh, M., Venkataswamy, M., Raju, B. D. P., & Sushma, N.
J. (2020). Synthesis And Characterization Of Curcumin Loaded Magnesium
Oxide Nanoparticles : Ph Dependent Invitro Release Behavior Of Loaded
Curcumin And Its Antioxidant Activity. *International Journal of Scientific &
Technology Research*, 9(2), 2151-2156.

Taylor, T. A., & Unakal, C. G. (2019). *Staphylococcus Aureus*. Stat Pearls Publishing:
Treasure Island (FL). Pp. 20-24.

Thern, A., Wastfelt, M., & Gunnar, L. (2020). Expression of Two Different Anti
phagocytic M Proteins by Streptococcus pyogenes of the OF$^+$ Lineage. *The
Journal Immunology,* 160, 860-869.

Umar, N. M., ivam, T. P., Aminu, N., & Toh, S. M. (2020). Phytochemical and
pharmacological properties of Curcuma aromatica Salisb (wild turmeric). *Journal
of Applied Pharmaceutical Science*, *10*(10), 180-194.

Vasanthan, K., Vengadakrishnan, K., & Surendran, P. (2018). Clinical Profile of Diabetic
Foot Infections. *International Journal of Scientific Study,* 6(1), 24-27.

Venkatasubbu, G. D., & Anusuya, T. (2017). Investigation on Curcumin nanocomposite
for wound dressing. *International Journal of Biological Macromolecules*, 98,
366-378.

Verma, R. K., Preeti, K., Rohit, K. M., Vijay, K., Verma, R. B., & Rahul, K. S. (2018).
Medicinal properties of turmeric (*Curcuma longa* L.): A review. *International
Journal of Chemical Studies,* 6(4), 1354-1357.

Vestby, L. K., Gronseth, T., Simm, R., & Nesse, L. (2020). Bacterial Biofilm and its Role
in the Pathogenesis of Disease. *Antibiotics*. 9(2), 59-65.

Wanigasekara, J., & Witharana, C. (2016). Applications of Nanotechnology in Drug
Delivery and Design - An Insight. *Current Trends in Biotechnology and
Pharmacy*, 10(1), 78-91.

World Health Organization. (2018). *E. coli.*

Wubante, D., Adinew, G. M., & Asrade, S. (2018). Evaluation of the Wound Healing Activity of the Crude Extract of Leaves of *Acanthus polystachyus Delile (Acanthaceae). Evidence-Based Complementary and Alternative Medicine*, 23, 1-9.

Yazdanpanah, L., Morteza, N., & Sara, A. (2015). Literature review on the management of diabetic foot ulcer. *World Journal of Diabetes,* 6(1), 37-53.

Zhang, P., Jing, L., Yali, J., Sunyi, Y. T., Dalong, Z., & Yan B. (2017). Global epidemiology of diabetic foot ulceration: A systematic review and meta-analysis. *Annals of Medicine,* 49(2), 1-11.

Appendix A

Minimum Inhibitory Concentration of Ethanol extract-mediated Silver Nanoparticles against Test Isolates.

	Concentration (mg/ml)						
Isolates	200	100	50	25	12.5	6.25	MIC
Klebsiella pneumoniae	+	+	+	+	+	-	12.5
Streptococcus pyogenes	+	+	+	+	+	-	12.5
Pseudomonas aeruginosa	+	+	+	+	-	-	25.0
Escherichia coli	+	+	+	-	-	-	50.0

+: Activity   -: No activity   mg/ml: milligram per millilitre

Appendix B

Minimum Inhibitory Concentration of Aqueous fraction-mediated Silver Nanoparticles against Test Isolates

Isolates	Concentration (mg/ml)						MIC
	200	100	50	25	12.5	6.25	
Klebsiella pneumoniae	+	+	+	+	+	-	12.5
Streptococcus pyogenes	+	+	+	+	+	-	12.5
Pseudomonas aeruginosa	+	+	+	+	-	-	25.0
Escherichia coli	+	+	+	+	+	-	12.5

+: Activity   -: No activity   mg/ml: milligram per millilitre

Appendix C

Minimum Inhibitory Concentration of Ethyl acetate fraction-mediated Silver Nanoparticles against Test Isolates.

Isolates	Concentration (mg/ml)						
	200	100	50	25	12.5	6.25	MIC
Klebsiella pneumoniae	+	+	+	+	+	-	12.5
Streptococcus pyogenes	+	+	+	+	+	-	12.5
Pseudomonas aeruginosa	+	+	+	+	+	-	12.5
Escherichia coli	+	+	+	+	+	-	12.5

+: Activity   -: No activity   mg/ml: milligram per millilitre

Appendix D

Minimum Inhibitory Concentrations of Chloroform fraction-mediated Silver Nanoparticles against Test Isolates

Isolates	Concentration (mg/ml)						
	200	100	50	25	12.5	6.25	MIC
Klebsiella pneumoniae	+	+	+	+	-	-	25.0
Streptococcus pyogenes	+	+	+	+	+	-	12.5
Pseudomonas aeruginosa	+	+	+	+	-	-	25.0
Escherichia coli	+	+	+	+	+	-	12.5

+: Activity   -: No activity   mg/ml: milligram per millilitre